INTRODUCTION TO KINETIC MODELING IN LOW-TEMPERATURE PLASMAS

Igor D. Kaganovich
Princeton Plasma Physics Laboratory, USA

PPPL
PRINCETON
PLASMA PHYSICS
LABORATORY

OUTLINE

Motivation: Needs of semiconductor production equipment makers

Nonlocal, nonlinear electron kinetics

Examples of control of electron, ion and photon distribution functions

Conclusions

The treatment has to be kinetic!

- Most remote from thermodynamic equilibrium:
  - T_e differs from T_i

3eV	**3 10^{-2} eV**	**glow discharges**
3 10^{-3} eV	**3 10^{-2} eV**	**afterglow**
10keV	**1eV**	**ECR ion sources**

- Electron energy distribution functions are nonMaxwellian:
  - Parts of the EDF are very flexible and almost independent.

Plasma parameters

- Plasma density $n = 10^9 - 10^{13}$ cm^{-3}
- Gas pressure = few mTorr
- Small degree of ionization $< 10^{-4}$
- Electron temperature T_e = few eV
- Ion temperature $T_i = 0.03$ eV
- Spatial scale = mm- m

GLOBAL MODEL: PARTICLE BALANCE DETERMINES T_e

Assuming steady-state and a Maxwellian Electron Energy Distribution Function =>

- Rate of plasma production = rate of plasma loss,
- Ionization frequency = loss frequency to the wall

$$\nu_{iz}(T_e) = \nu_{loss}(T_e)$$

$$\nu_{iz} = n_g V_T \sigma_{iz} e^{-I/T_e},$$

$$\nu_{loss} = \gamma C_s / L \quad C_s = \sqrt{T_e / M}$$

$$n_g V_T \sigma_{iz} e^{-I/T_e} = \gamma \frac{\sqrt{T_e / M}}{L}$$

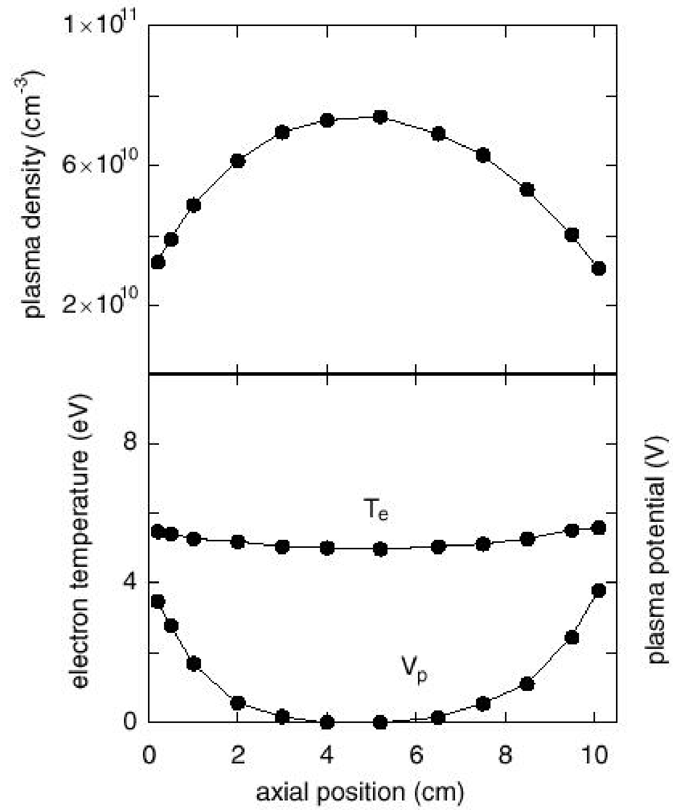

V. GODYAK'S EXPERIMENT IS BENCHMARK.

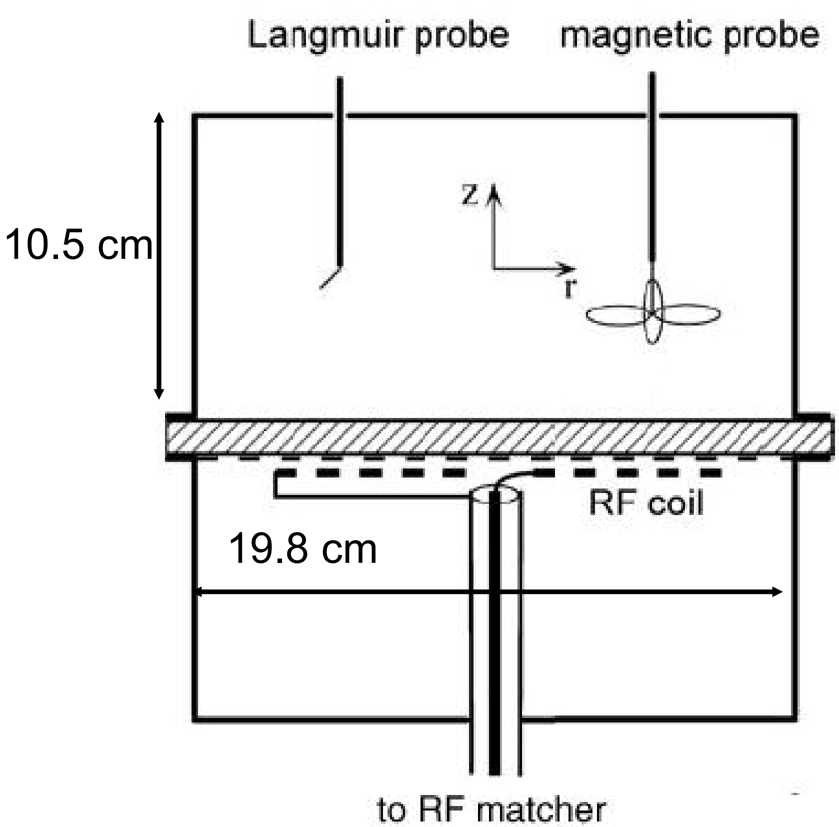

Figure 1. Experimental discharge chamber.

The Inductively Coupled Plasmas (ICP)
f=0.45-13.56 MHz
argon gas pressures 0.3-300 mTorr
rf power 6-400 W.

V. A. Godyak, R. B. Piejak, and B. M. Alexandrovich, J. Appl. Phys. **85**, 703 (1999).

EXPERIMENT (LEFT) AND GLOBAL MODEL (RIGHT) GIVE CLOSE AGREEMENT

$$n_g V_T \sigma_{iz} e^{-I/T_e} = \gamma \frac{\sqrt{T_e / M}}{L} \quad \uparrow n_g L \ \downarrow T_e$$

T_e as a function of gas pressure at f=6.78 MHz

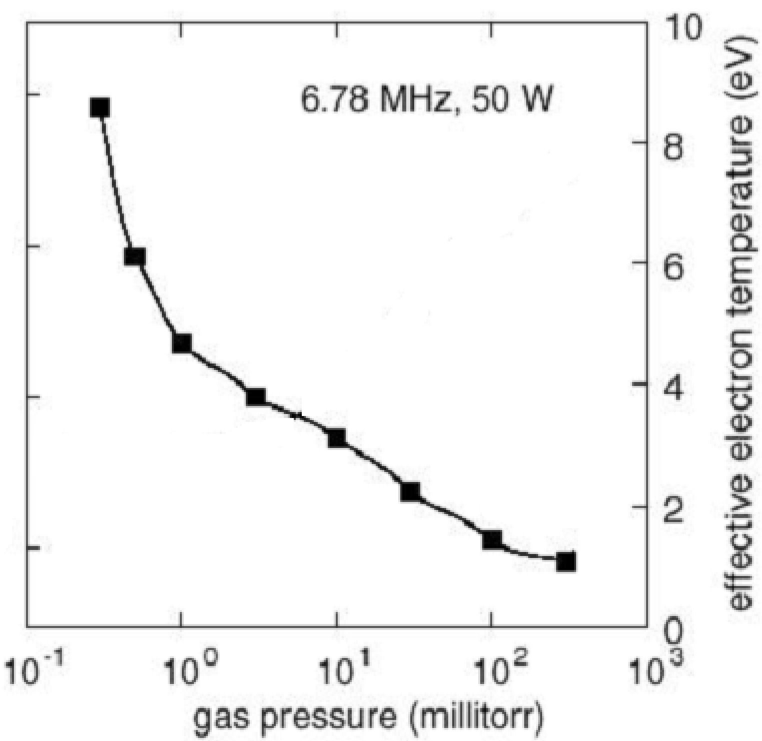

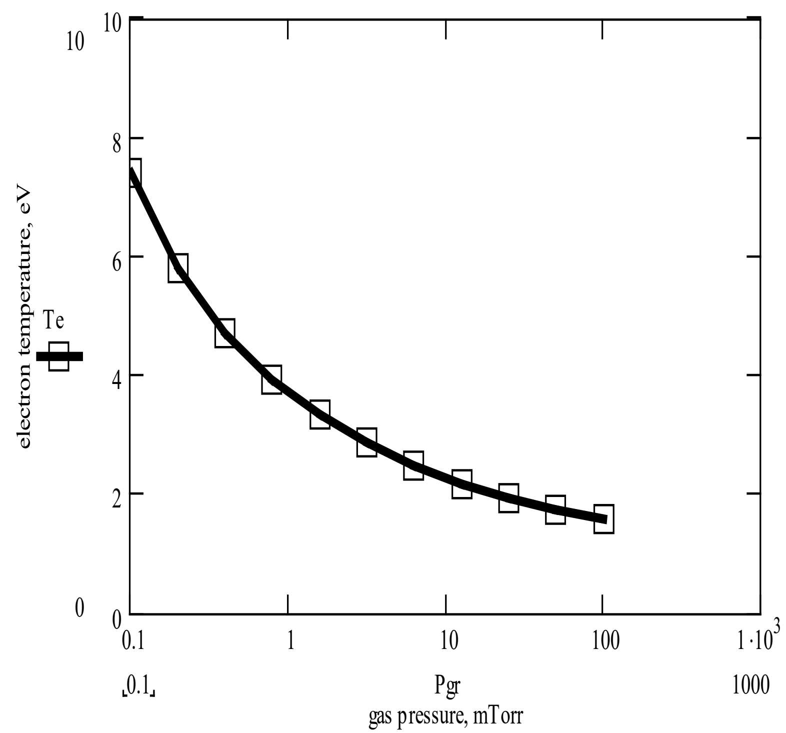

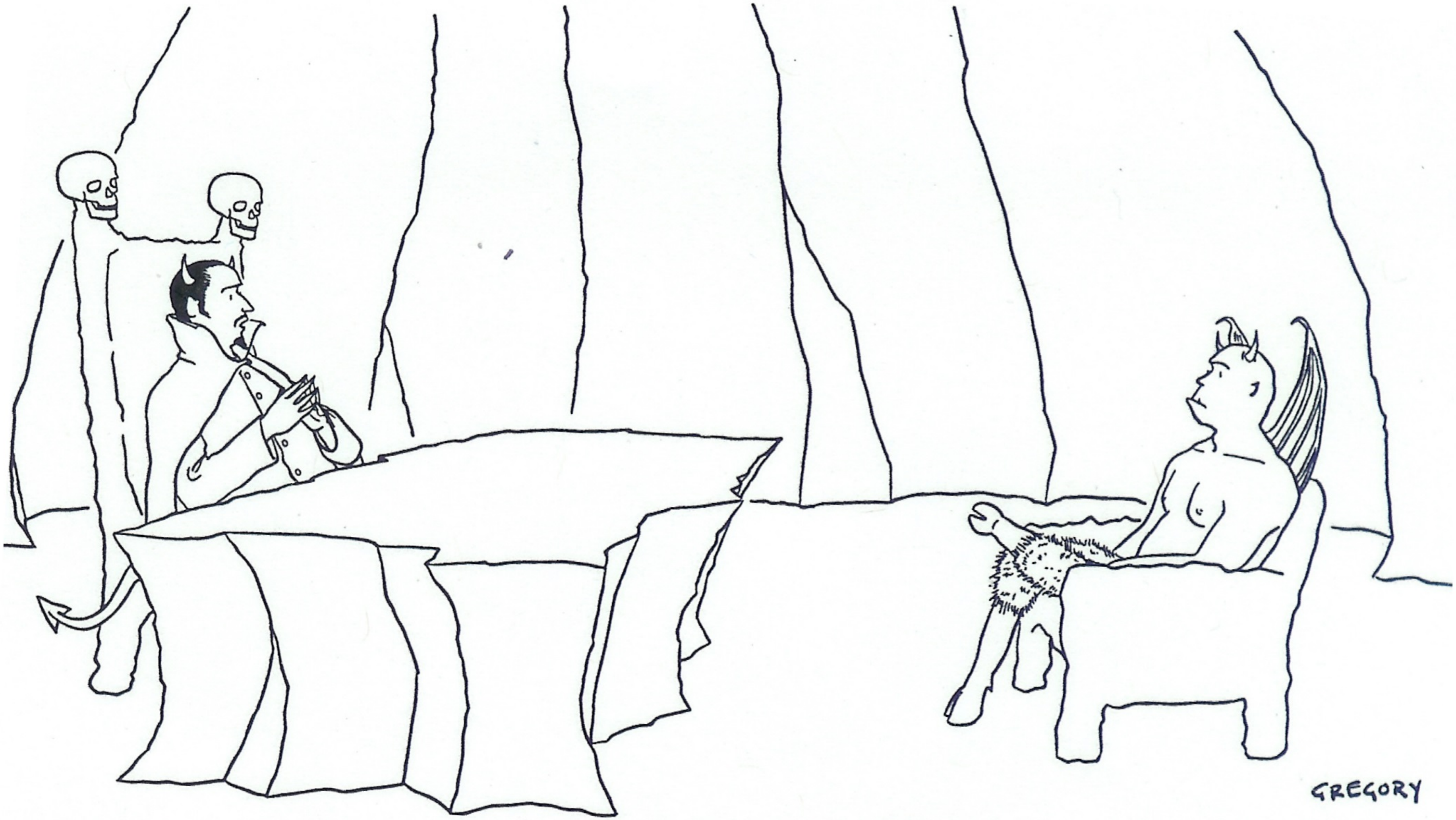

"I need someone well versed in the art of torture—do you know PowerPoint?"

$$J = \frac{\partial E}{4\pi \partial t} + \sigma E$$

TABLE 1.1. Range of Parameters for rf Diode and High-Density Discharges

Parameter	rf Diode	High-Density Source
Pressure p (mTorr)	10–1000	0.5–50
Power P (W)	50–2000	100–5000
Frequency f (MHz)	0.05–13.56	0–2450
Volume $\mathcal{V}$ (L)	1–10	2–50
Cross-sectional area A (cm^2)	300–2000	300–500
Magnetic field B (kG)	0	0–1
Plasma density n (cm^{-3})	10^9–10^{11}	10^{10}–10^{12}
Electron temperature T_e (V)	1–5	2–7
Ion acceleration energy $\mathcal{E}_i$ (V)	200–1000	20–500
Fractional ionization x_{iz}	10^{-6}–10^{-3}	10^{-4}–10^{-1}

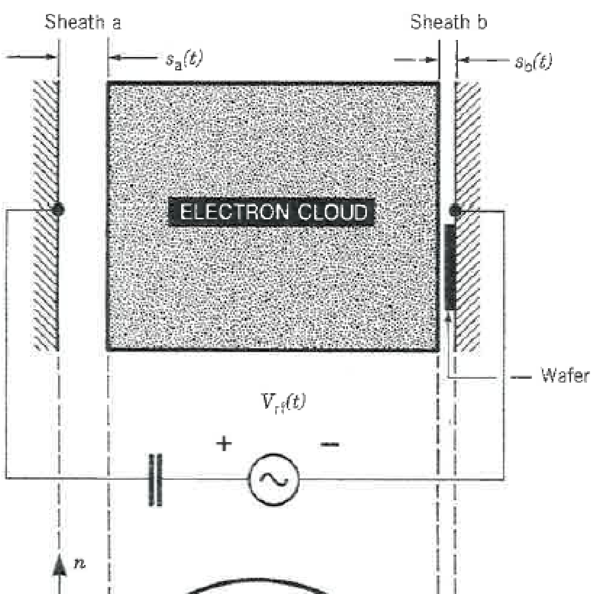

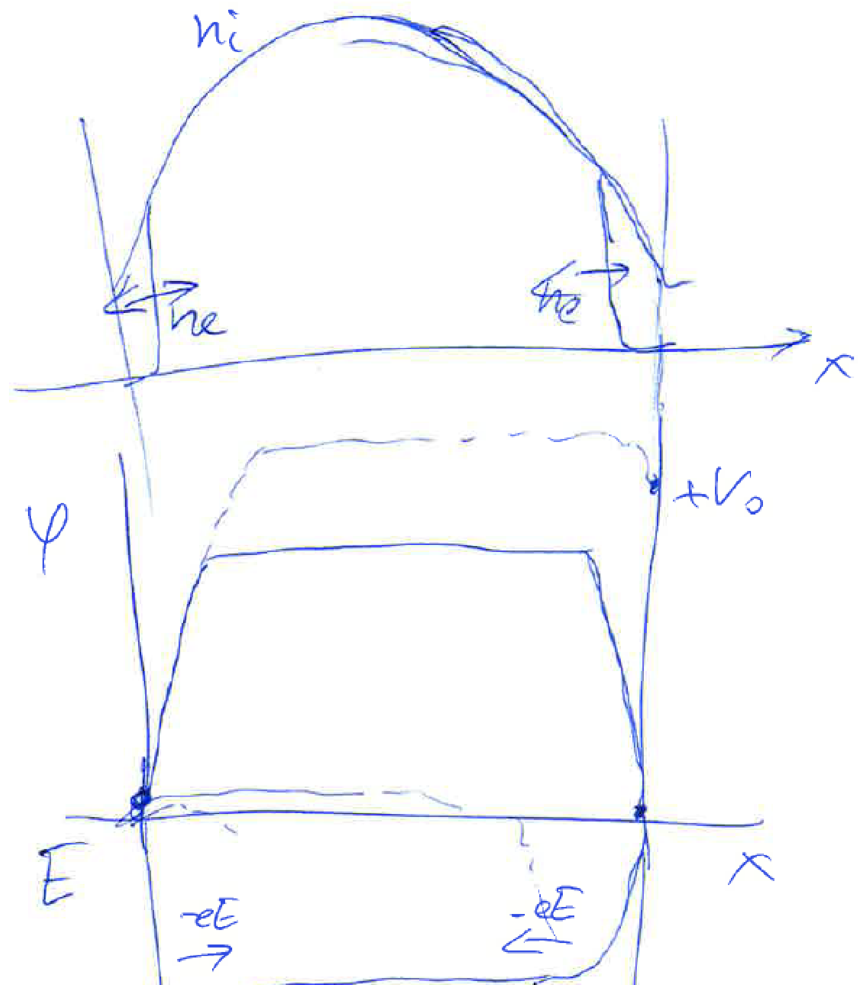

DISCHARGE MODELING NEEDS TO BE KINETIC!

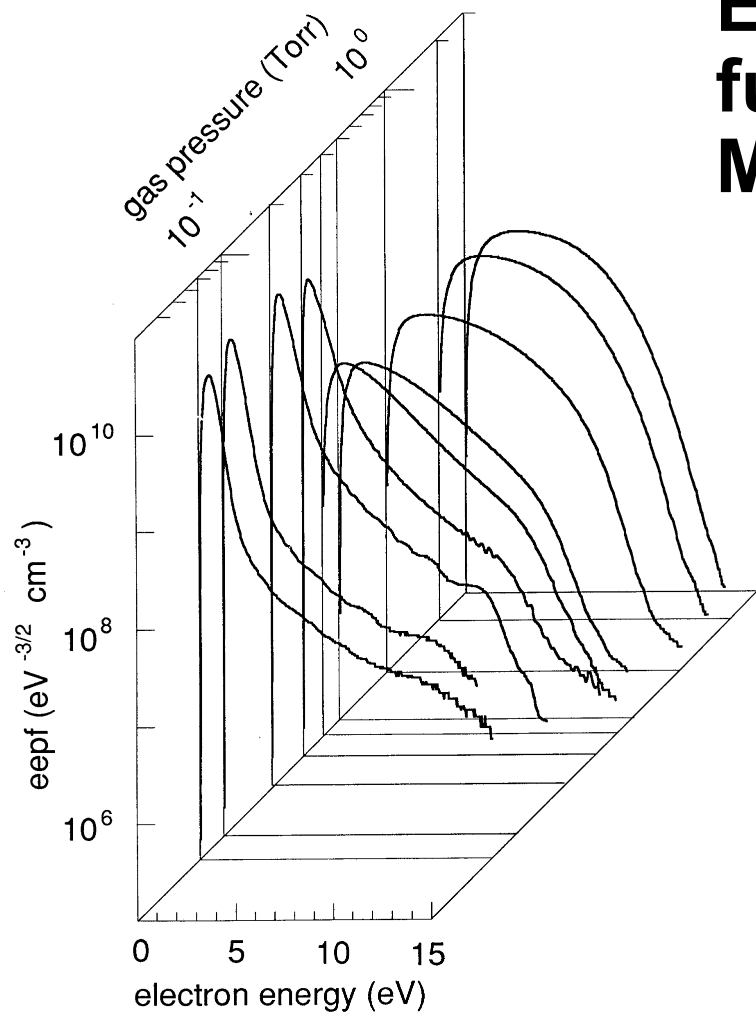

Electron energy distribution functions (EEDF) are non-Maxwellian:

- **Parts of the EEDF are very flexible and almost independent.**
- **An example of a EEDF in capacitive discharge.**

For more info: **V. Godyak, IEEE TPS 34, 755 (2006).**

MECHANISM OF EEDF FORMATION
II. COOLING AND MIXING

Cooling is due to energy losses in elastic and inelastic collisions.

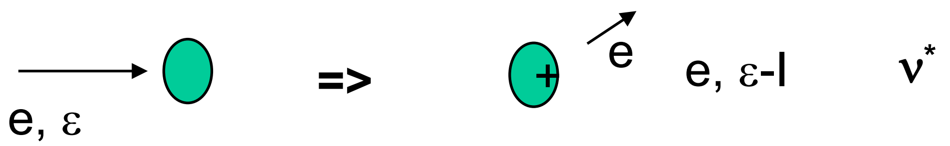

Mixing is due to electron-electron collisions.

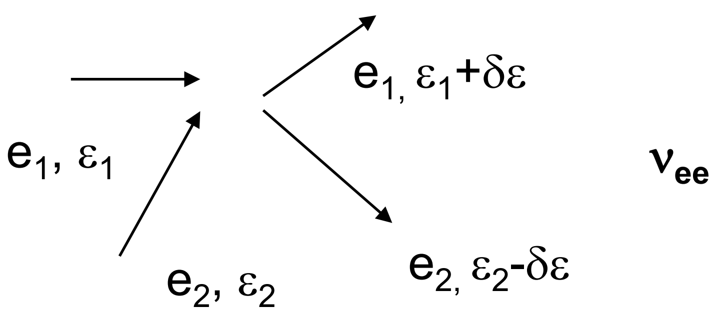

It is the only mechanism to make EEDF a Maxwellian! =>
If $\nu_{ee} >> \nu^*$ EEDF is a Maxwellian; degree of ionization $n_e/n_g > 10^{-4}$
If $\nu_{ee} << \nu^*$ EEDF can be anything, $n_e/n_g < 10^{-4}$

NONLOCAL, NONLINEAR ELECTRON KINETICS

- **Formation of non-Maxwellian, non-uniform, *f(v,r,t)* in self-consistent electric field strongly coupled to plasma density profile through ionization and transport for realistic discharge plasmas.**

$$\left[\frac{\partial}{\partial t}+(\mathbf{v}\nabla)-e\mathbf{E}\frac{\partial}{m\partial\mathbf{v}}\right]f=\sum_k\left[\nu_k^{*}{}'\frac{\sqrt{u'}}{\sqrt{u}}f(w+w_k^*)-\nu_k^* f\right]+St_{ee},$$

$$\frac{\partial n_i}{\partial t}+\nabla(\mathbf{v}n_i)=\nu_{iz}n_i,\quad \nu_{iz}n_i=\int_I^\infty f(u)v\sigma_{iz}d\mathbf{v}$$

$$\nabla\mathbf{E}=4\pi e(n_i-n_e)$$

$$M_i\left(\frac{\partial\mathbf{v}}{\partial t}+(\mathbf{v}\nabla)\mathbf{v}\right)=e\mathbf{E}-\frac{\nabla p_i}{n_i}-(\nu_{ia}+\nu_{iz})\mathbf{v}$$

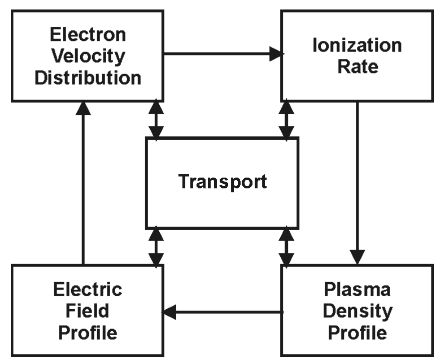

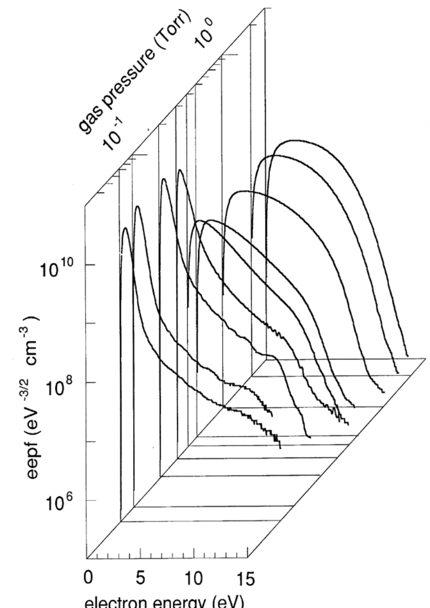

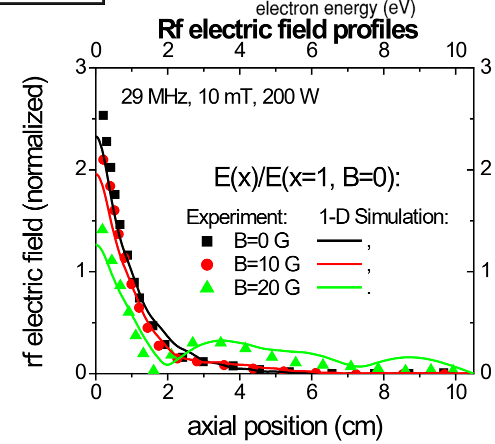

- **Igor D. Kaganovich et al, Phys. Rev. Lett. 1999, 2000, 2002, 2009, 2012, 2013;**
- **Valery Godyak et al, Phys. Rev. Lett. 1990,1992, 1996, 1998, 1999.**

MECHANISM OF EEDF FORMATION
1. HEATING

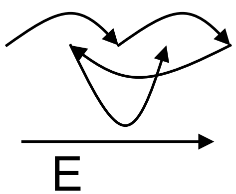

Elastic collisions with mean free path λ =>
Random space diffusion yields =>
Diffusion in energy with energy kick eEλ

$$\frac{\partial f_0}{\partial t} = \frac{\partial}{\sqrt{\varepsilon}\partial\varepsilon}\left(\sqrt{\varepsilon}D_{\varepsilon}(\varepsilon)\frac{\partial f_0}{\partial\varepsilon}\right)$$

$$P = -\int_0^{\infty}\sqrt{\varepsilon}D_{\varepsilon}(\varepsilon)\frac{\partial f_0}{\partial\varepsilon}d\varepsilon$$

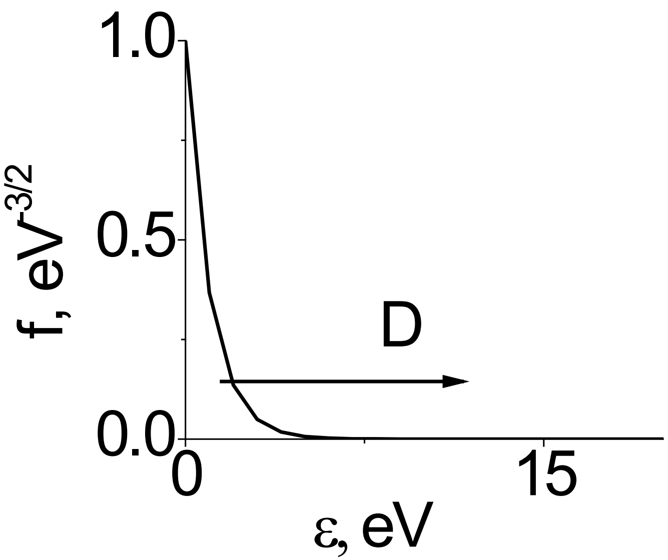

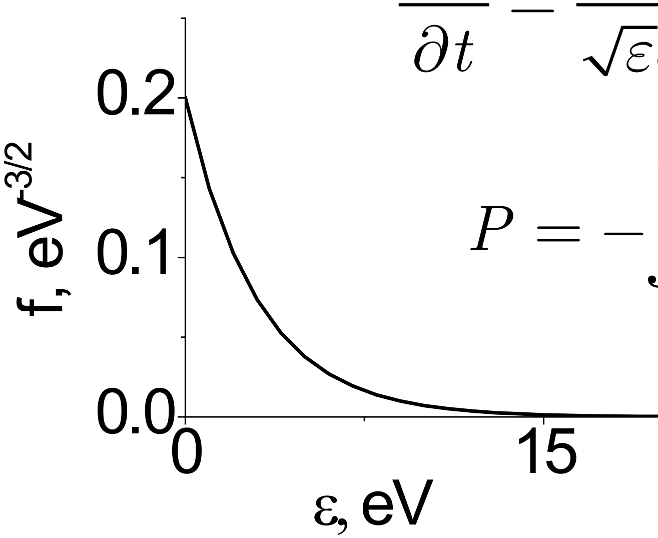

Diffusion in energy leads to heating

EEDF IN NITROGEN, CONSTANT ELECTRIC FIELD

1930 Druyvesteyn's EEDF for λ constant.

$$f \sim \exp(-\varepsilon^2/\varepsilon^2_0)$$

Real cross-sections in N_2

N.L. Alexandrov, *et al*. Sov. J. Plasma Phys. 1978

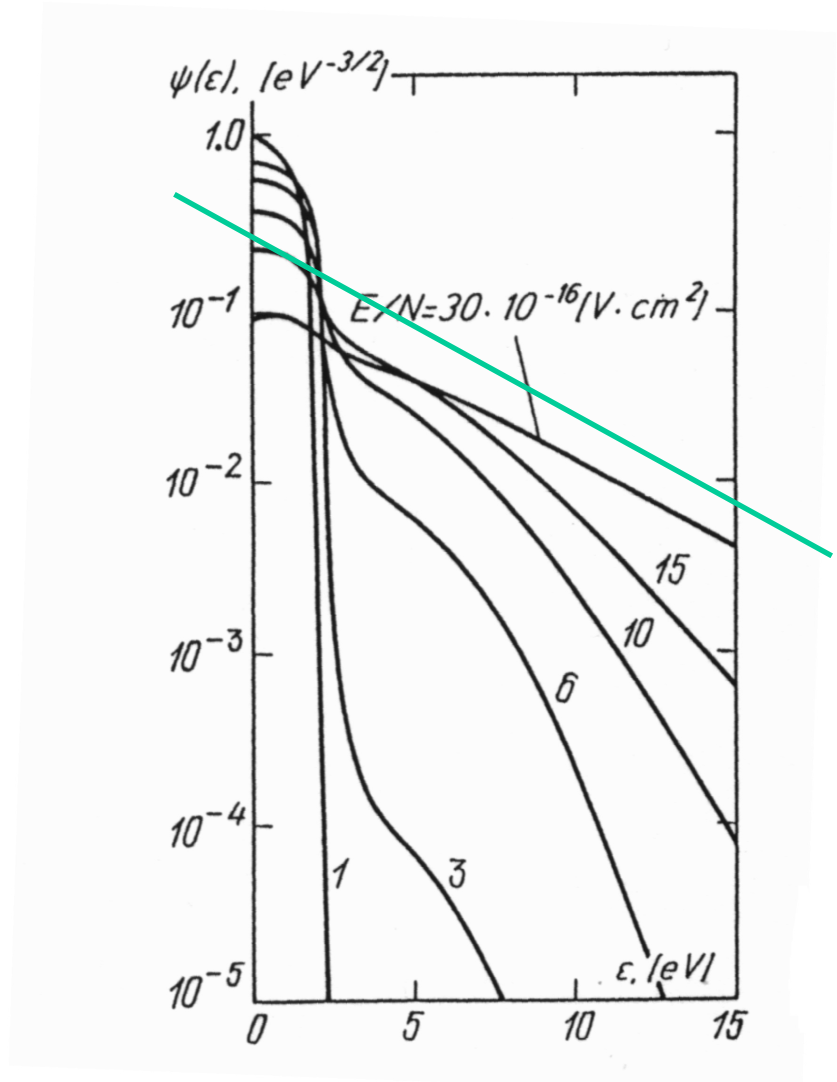

EEDF IN DECAYING PLASMA

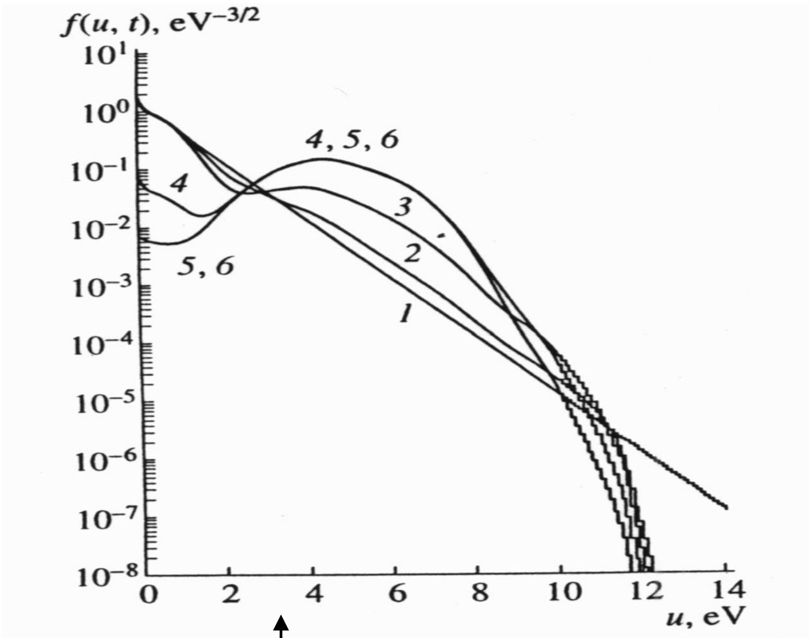

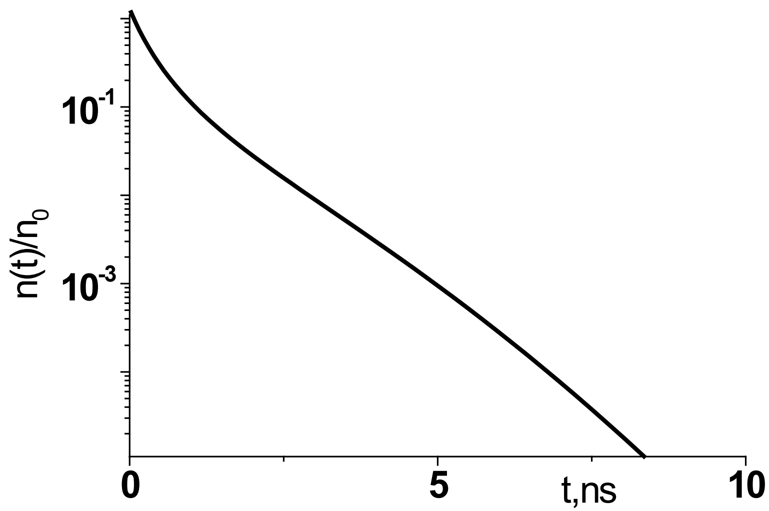

Strong energy losses

EEDF afterglow Ar:$NF_{3.}$ E/N=2 10^{-17}Vcm^2

- **1, 2, 3, 4, 5, 6.**
- **0, 0.25, 1, 3, 5, 10 ns.**

N.A. Dyatko, *et al.* Plasma Phys. Rep. 1998

Workshop Website: http://w3.pppl.gov/~ikaganov/PPPL2005/

Special Issue in IEEE Trans. Plasma Science 2006

NON-MONOTONIC EEDF YIELDS NEGATIVE PLASMA CONDUCTIVITY!

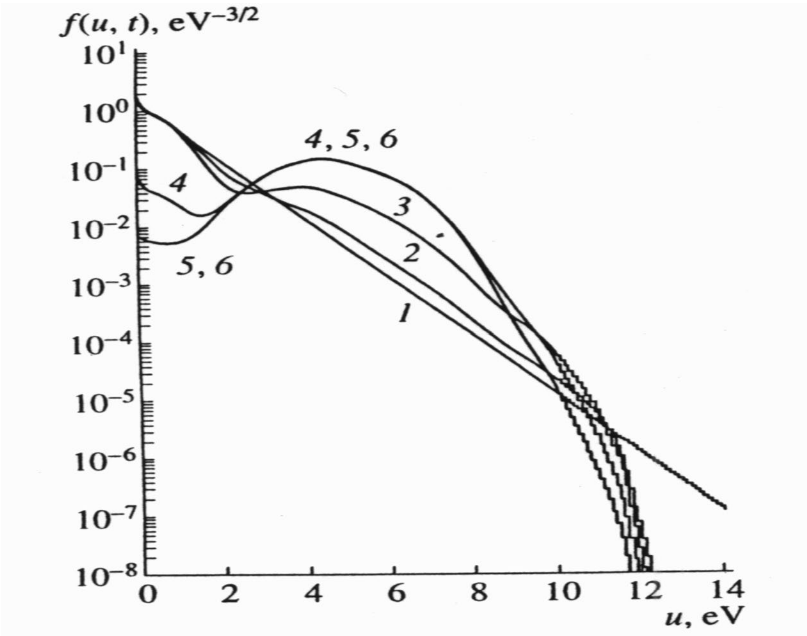

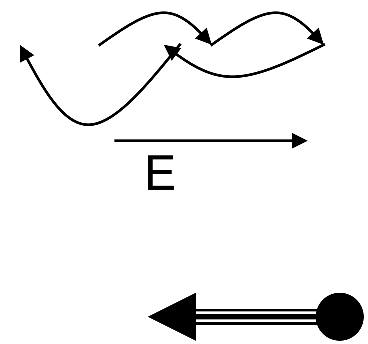

Total electron flux is opposite to the electric field

$$\mu = -\frac{2e}{3m}\int u^{1/2}\lambda\frac{df(u)}{du}du < 0 \qquad \frac{\partial f_0}{\partial t} = \frac{\partial}{\sqrt{\varepsilon}\partial\varepsilon}\left(\sqrt{\varepsilon}D_\varepsilon(\varepsilon)\frac{\partial f_0}{\partial \varepsilon}\right)$$

EVAPORATIVE ELECTRON COOLING IN AFTERGLOW

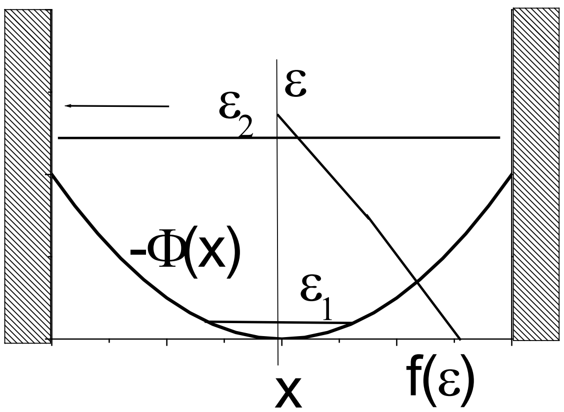

In non-uniform plasmas low-energy electrons are trapped, where as high-energy electrons can leave.
=>
T_e reduces when plasma decays

Electron temperature can cool to 30K!
Biondi (1954)

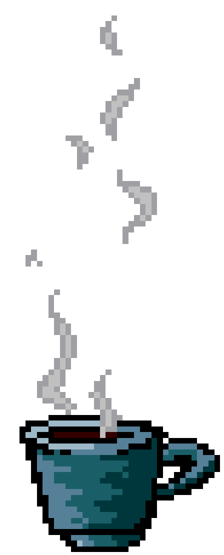

EVAPORATIVE ELECTRON COOLING IN AFTERGLOW

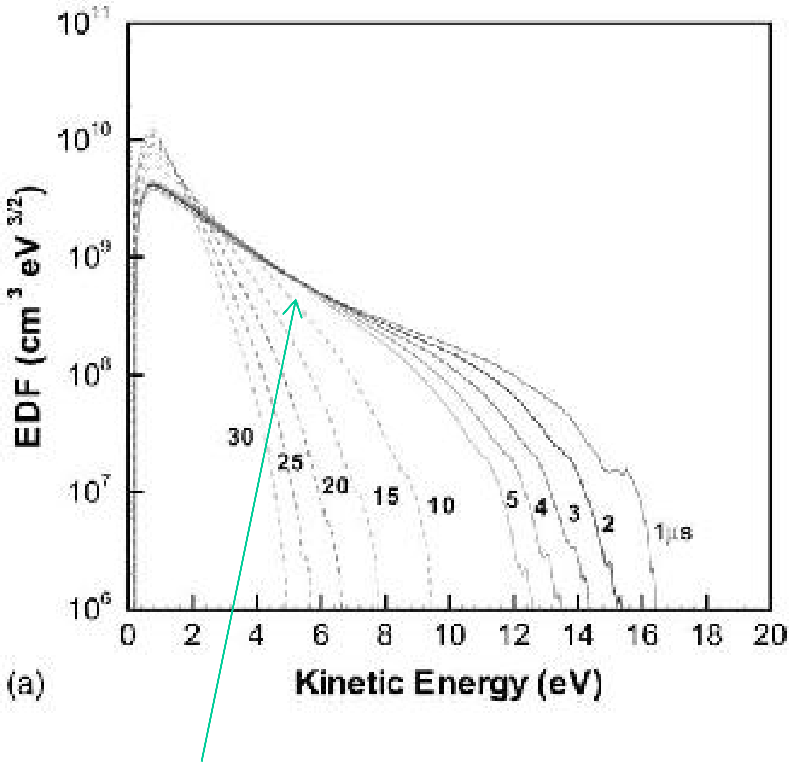

$\nu_{ee}\ \tau$=1

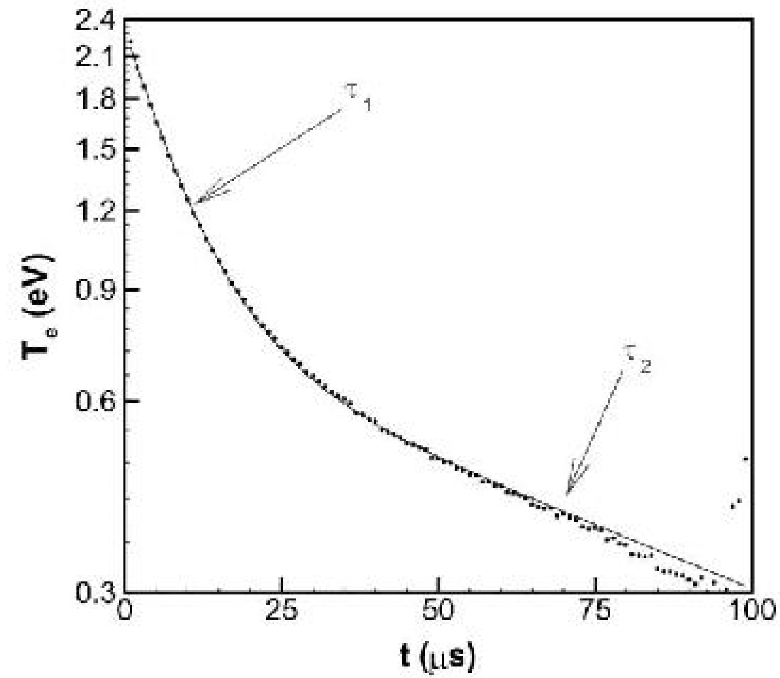

Fig. 7. Decay of the "electron temperature" at 15 mTorr.

Experiment: Kortshagen, *et al*. Appl. Surf. Sci. 192, 244 (2002)

EFFECTS OF PENNING IONIZATION IN AFTERGLOW

In the afterglow, electrons cool rapidly to T_e ~ 0.2 eV.

However, a small amount of fast electrons with energy few eV arise from slowly decaying metastables, due to, e.g., the Penning ionization ***$A^* + A^* \rightarrow A + A^+ + e_f$.***

He ε^*=20 eV I=25eV

$2\varepsilon^*$-I=2*20-25=15 eV

Experimental EEDF in He afterglow, V.I. Demidov (2005)

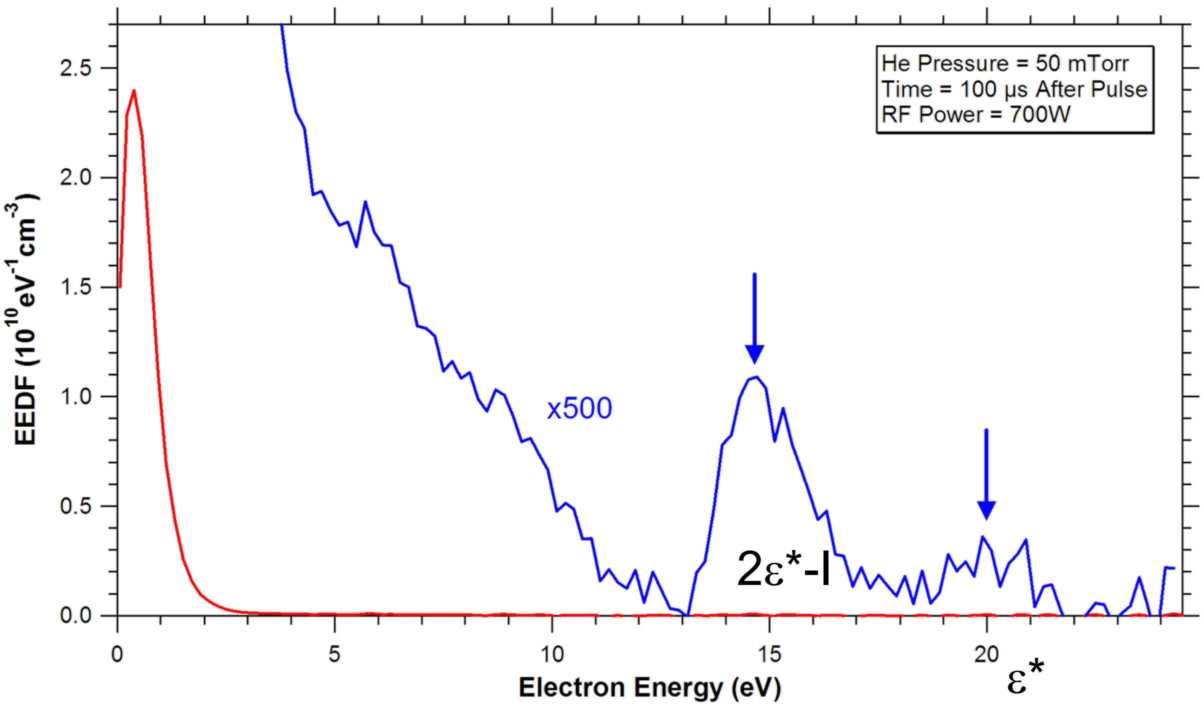

EFFECT OF A SMALL POPULATION OF FAST ELECTRONS ON WALL POTENTIAL (1)

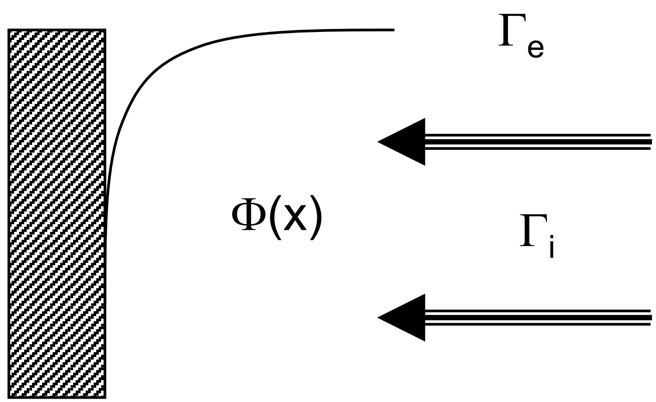

$$\Gamma_e = n\sqrt{\frac{T_e}{2\pi m}}e^{-\phi/T_e}$$

$$\Gamma_i = n\sqrt{\frac{T_e}{M}}$$

$$\Gamma_e = \Gamma_i$$

$$e\phi_p = T_e \ln\left(\sqrt{\frac{M}{2\pi m}}\right) \sim 5T_e$$

Relies on the assumption of a Maxwellian electron energy distribution function. Small flux of energetic electrons with $\Gamma_{ef} > \Gamma_i$ can strongly modify sheath.

EFFECT OF A SMALL POPULATION OF FAST ELECTRONS ON WALL POTENTIAL (2)

Afterglow in 0.2Torr Xe. Left - exp. T_e . Right - the wall potential: stars – exp. data, diamonds - 5T_e and squares – calculations.

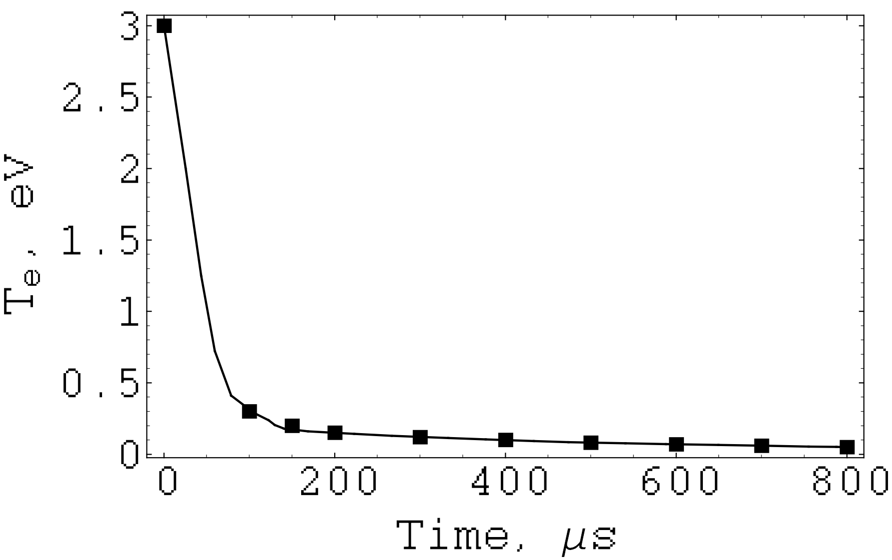

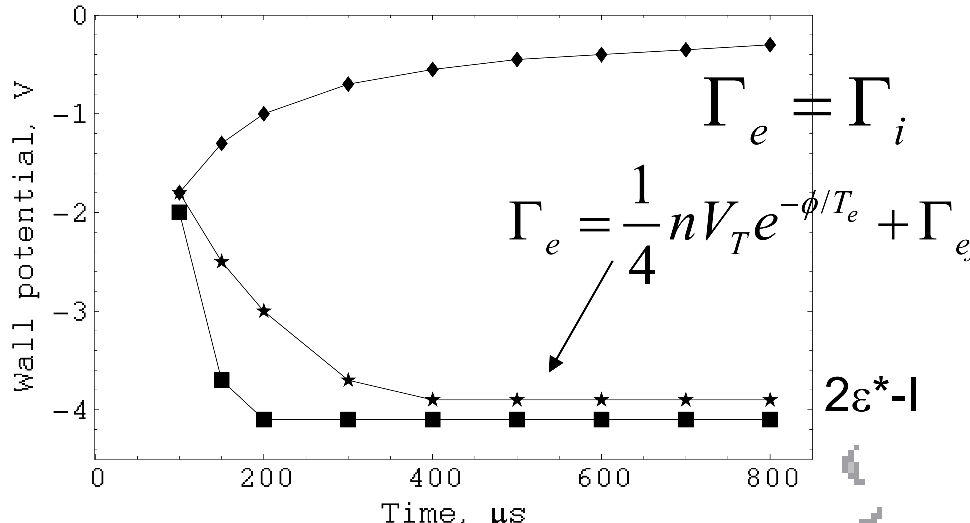

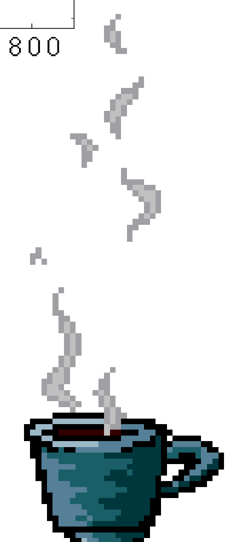

V.I. Demidov, et al, PRL 95, 215002 (2005).

Near-wall potential drop can be much greater than Te =>
This large wall potential can lead to an <u>increase</u> in electron density, diffusion cooling can be eliminated.

THE ABRUPT FORMATION OF LARGE POPULATION OF COLD ELECTRONS

- **Large population of cold electrons is typical in various glow discharges.**
- **“Paradoxical” electron cooling with power increase.**
- **Plasma density jumps with power increase.**

COLD ELECTRONS: EXPLANATION

- **Necessary conditions:**
  - **Non-locality**
  - **Non-linearity**

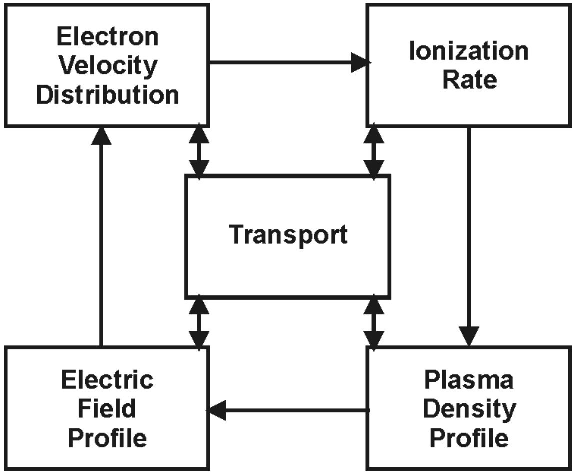

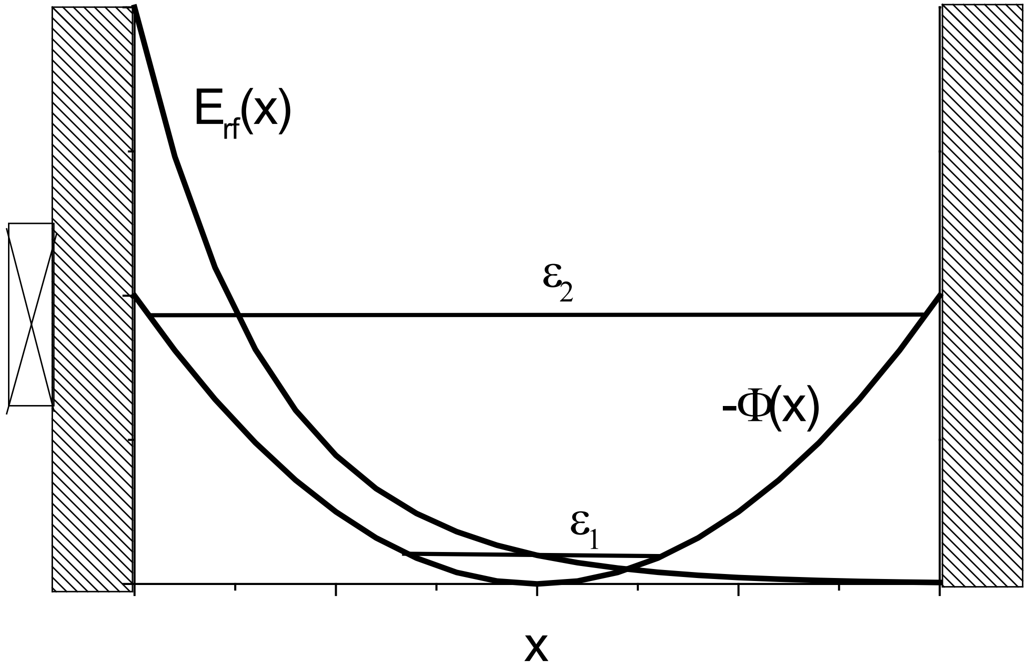

COLD ELECTRONS IN DC DISCHARGE

cathode $\xrightarrow{-eE}$ anode

cathode $\xrightarrow{-eE}$ anode

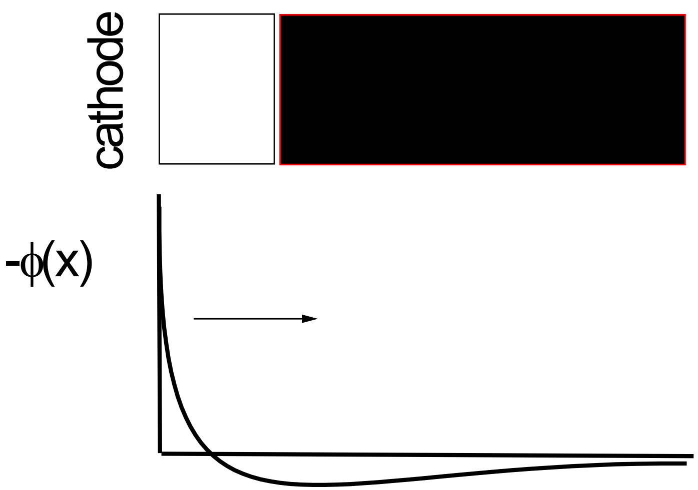

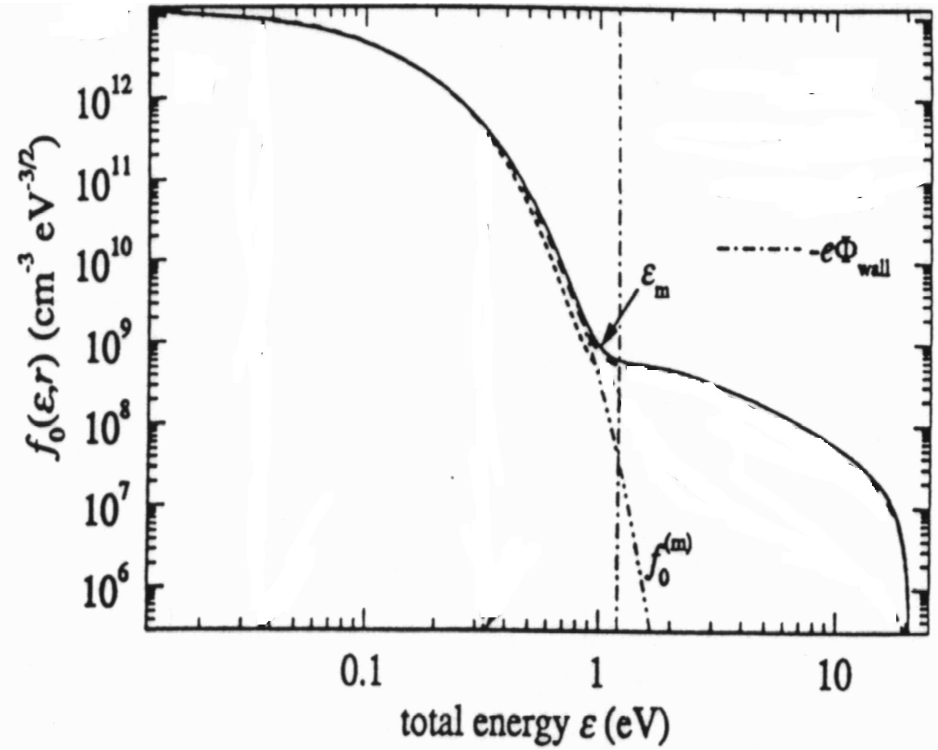

Cathode fall

He 3.5 Torr, 0.85mA/cm^2, 260V, 0.62cm

Exp.: T_e=0.12eV

E.A. Hartog et. al., PRL 1989

Model: R. Arslanbekov, A. Kudryavtsev PRE 1998

COLD ELECTRONS IN ECR DISCHARGE

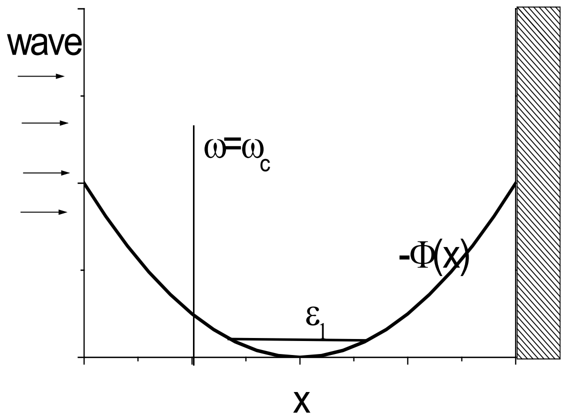

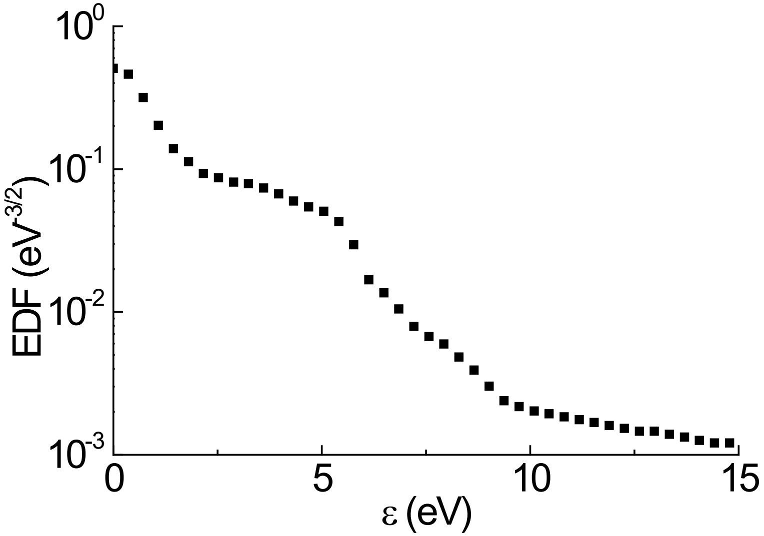

Electron cyclotron resonance discharge

- N_2 1mTorr, 0.14W/cm^2, 50cm
- Exp.: N. Bibinov, *et al.,* Rev. Sci. Ins. 1998, 2004
- Model.: I. Kaganovich *et al.* PRE 1999

COLD ELECTRONS: ICP

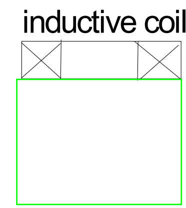

- **Inductively coupled discharge**
  - **Argon 1mtor,**
  - **Pancake geom. 20x10.5cm**
  - **V A Godyak & V I Kolobov PRL 1998**

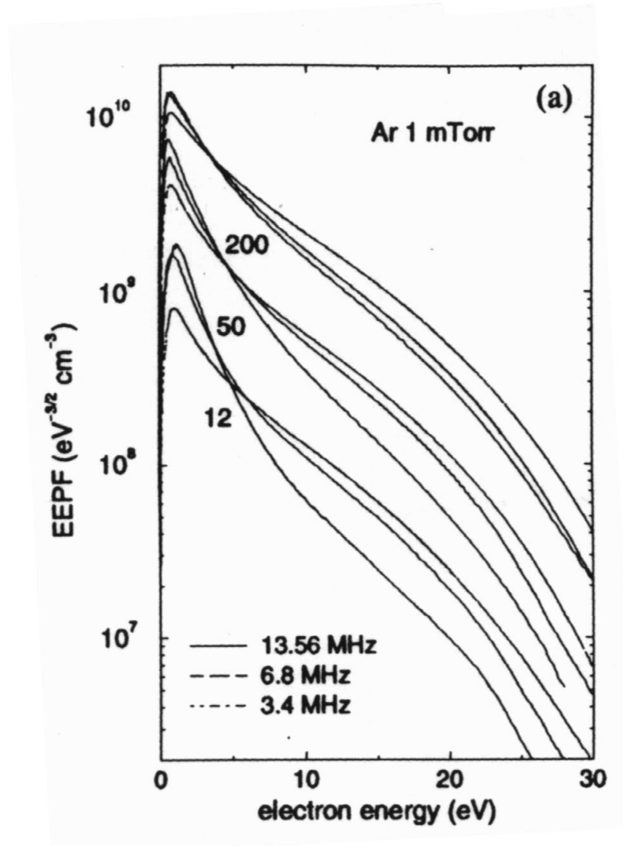

EXPLOSIVE GENERATION OF COLD ELECTRONS IN CAPACITIVE DISCHARGE

EEDF modification with discharge current

Argon,

13.56MHz, 6cm, 9Pa

U. Buddemeier et.al., APL (1996)

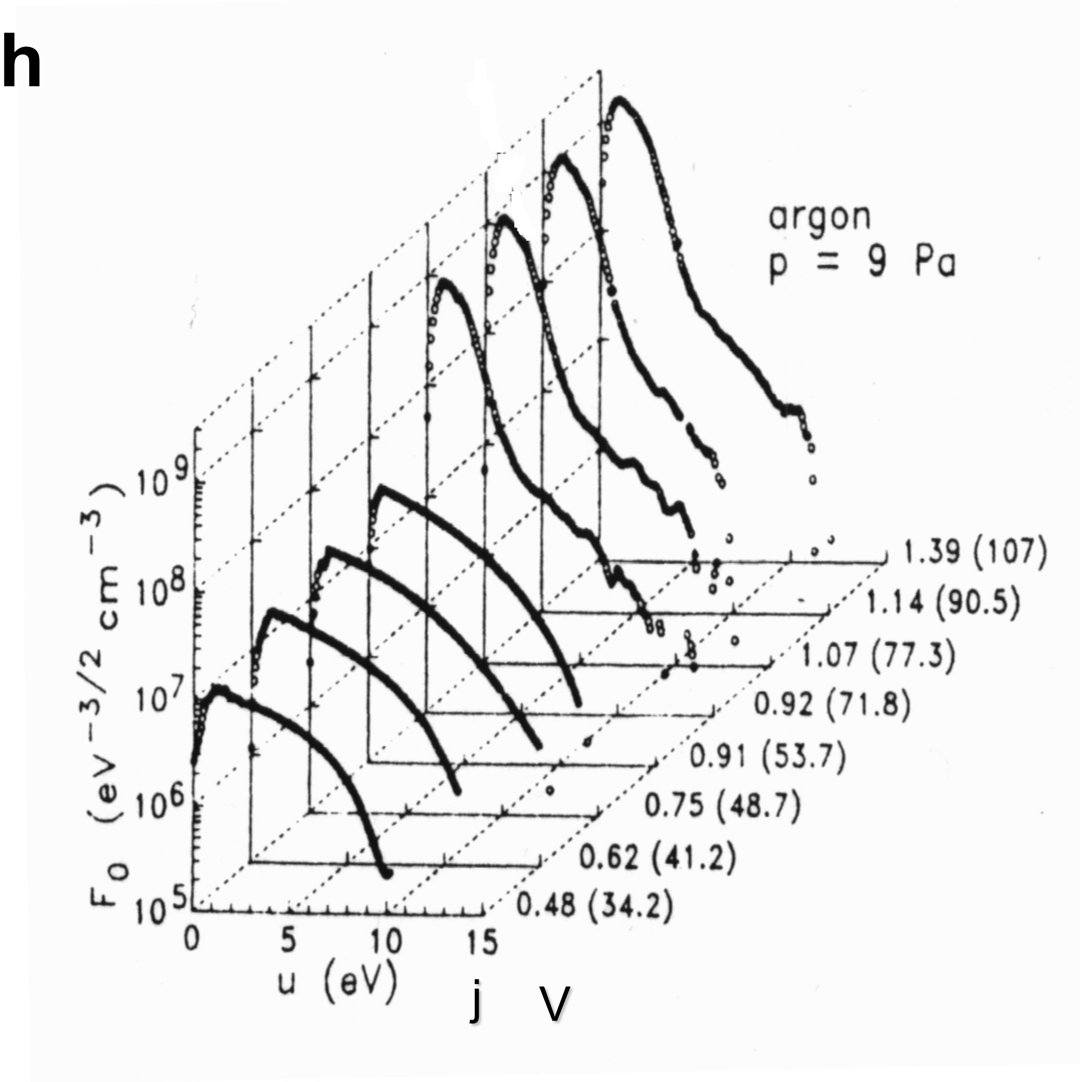

"ELECTRON REFRIGERATOR"

Plasma parameters evolution with current

Argon, 13.56mHz, 6.7cm, 0.1torr

Symbols: exp. V. Godyak *et. al*. Plasma Sci. & Technol. (1992)

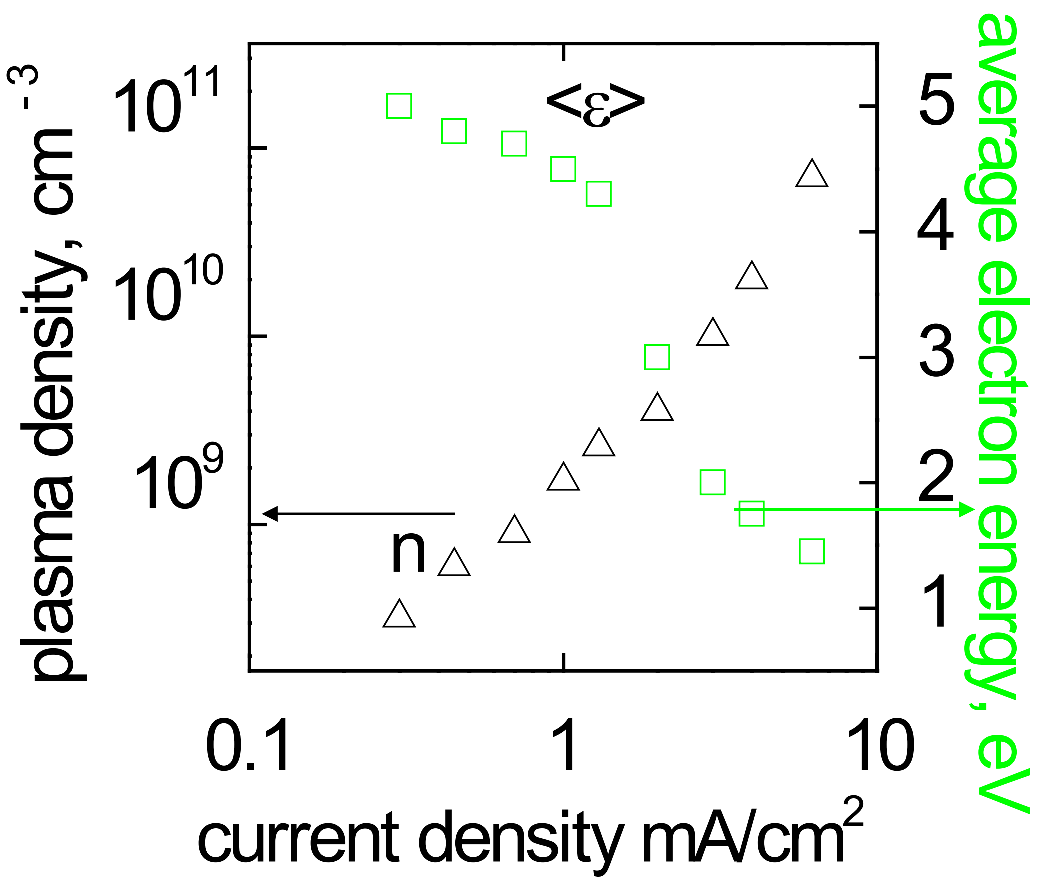

MODELING: ABSENCE OF STEADY STATE

The EDFs and ion density profiles at three subsequent times

Solid lines: e-e collisions are ignored. (1) t=0ms, (2) t=0.34ms, (3) t=2.24ms.

Dashed lines: with e-e collisions

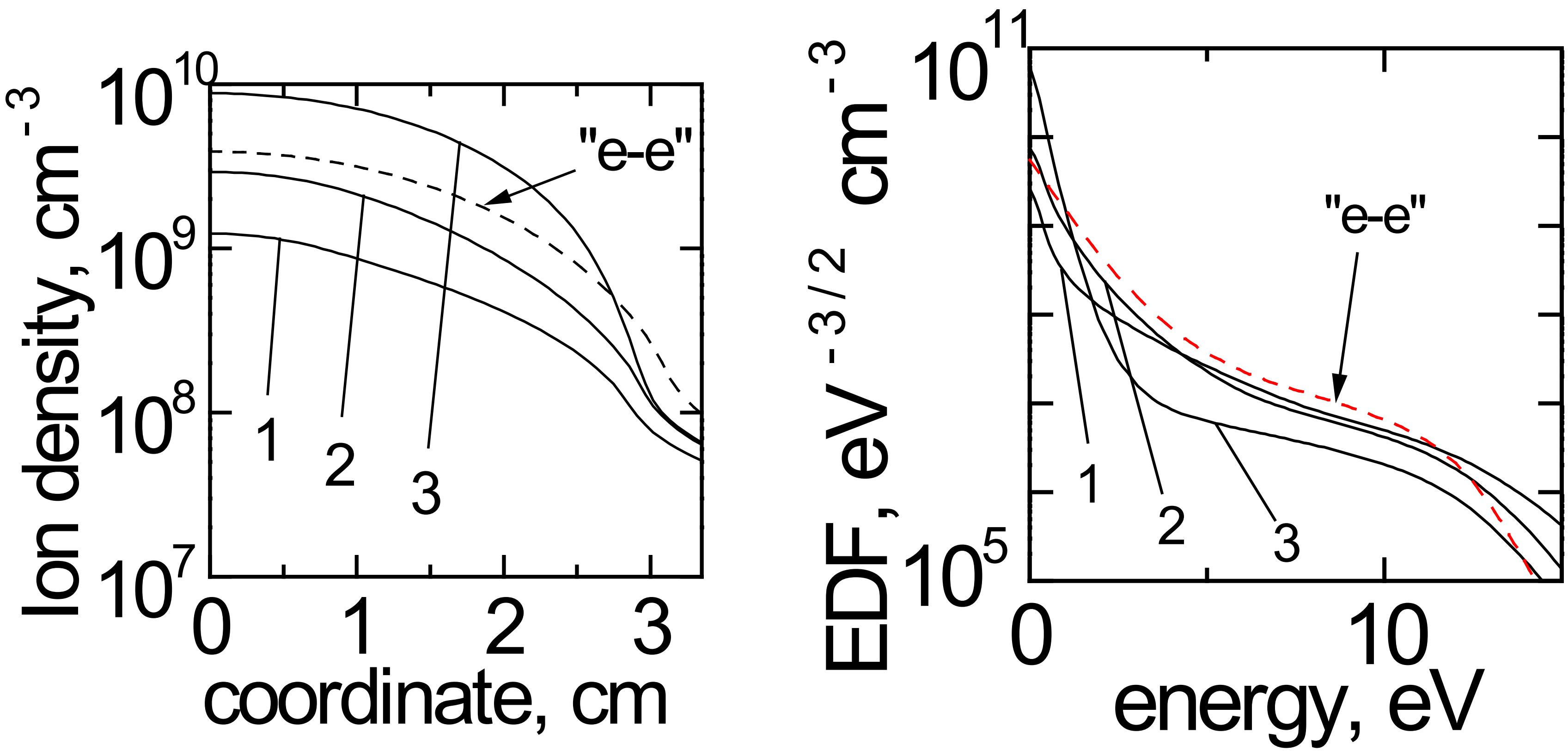

S.V. Berezhnoi, I.D. Kaganovich and L.D. Tsendin, Plasma Physics Reports **24**, 556 (1998).

NONLOCALITY IS IMPORTANT FOR MANY PLASMA APPLICATIONS

Electron energy relaxation length is large; this allows remote plasma handling via nonlocal electron energy distribution function (EEDF).

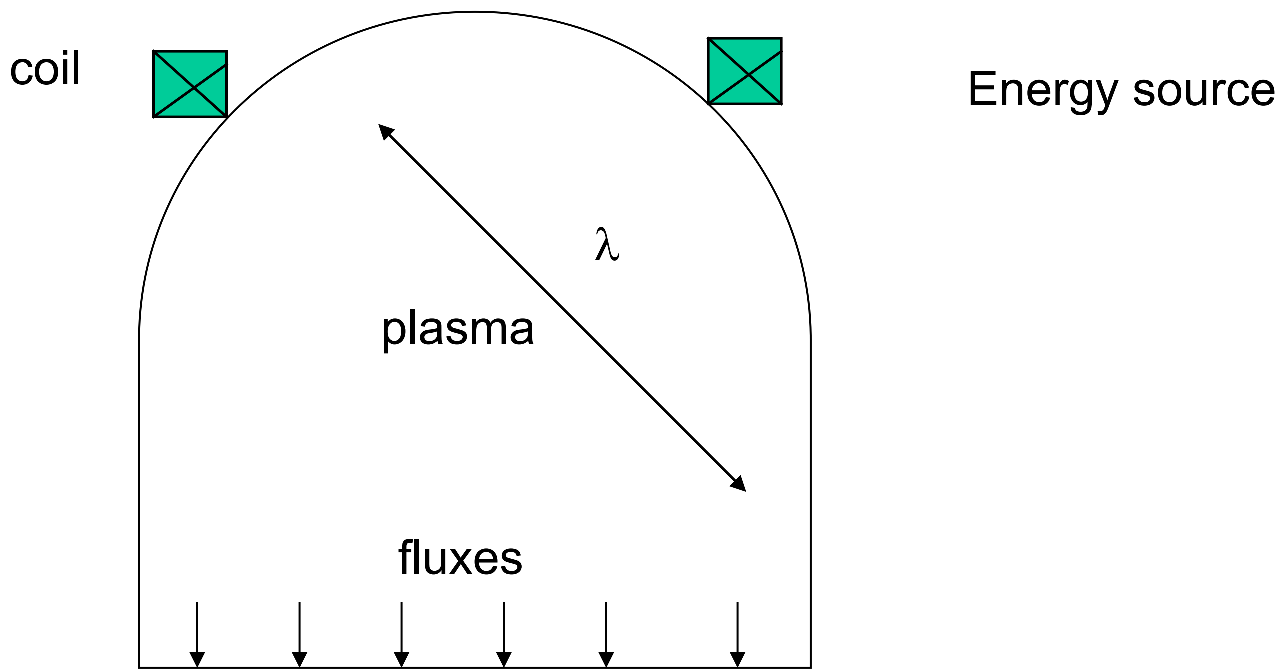

NONLOCAL APPROACH - AVERAGING OVER FAST ELECTRON BOUNCING

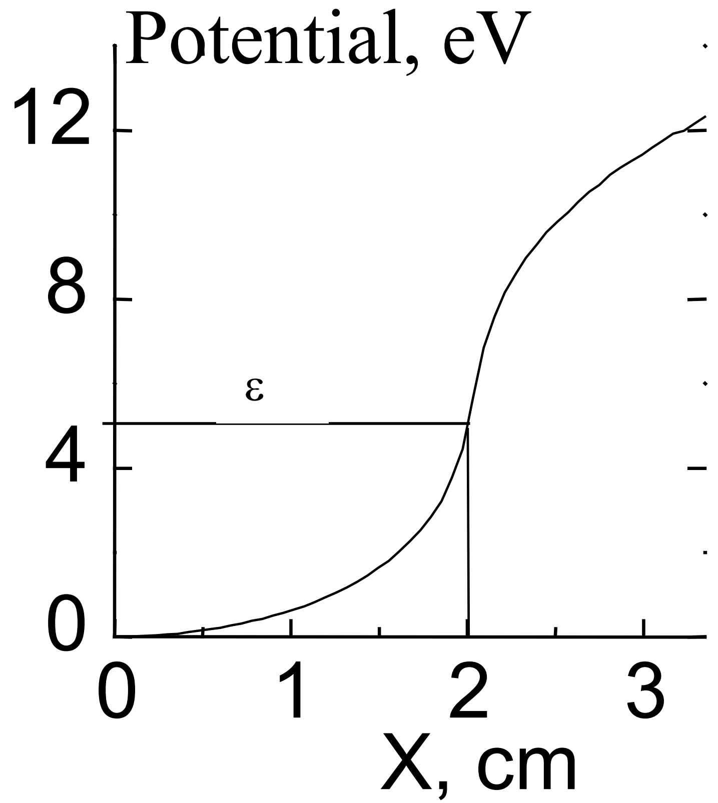

$$\varepsilon = \frac{mv^2}{2} + e\Phi(\vec{r})$$

$F(\varepsilon)$ **is the function of total energy only**

I.B. Bernstein, T. Holstein,
Phys. Rev. 94, 1475 (1954).
L.D. Tsendin,
Sov.Phys. - JETP, 39, 805 (1974).

NONLOCAL EEDF IS A FUNCTION OF TOTAL ENERGY $\varepsilon = mv^2/2 - e\varphi(x)$

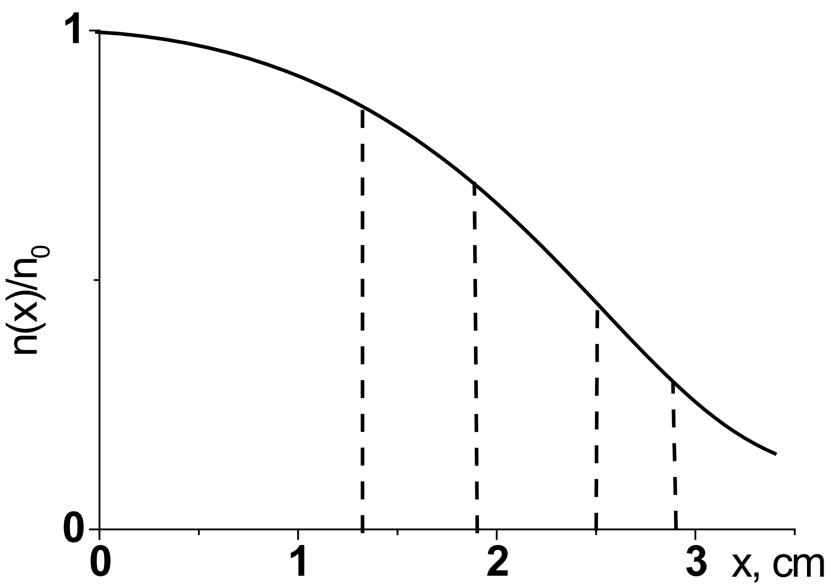

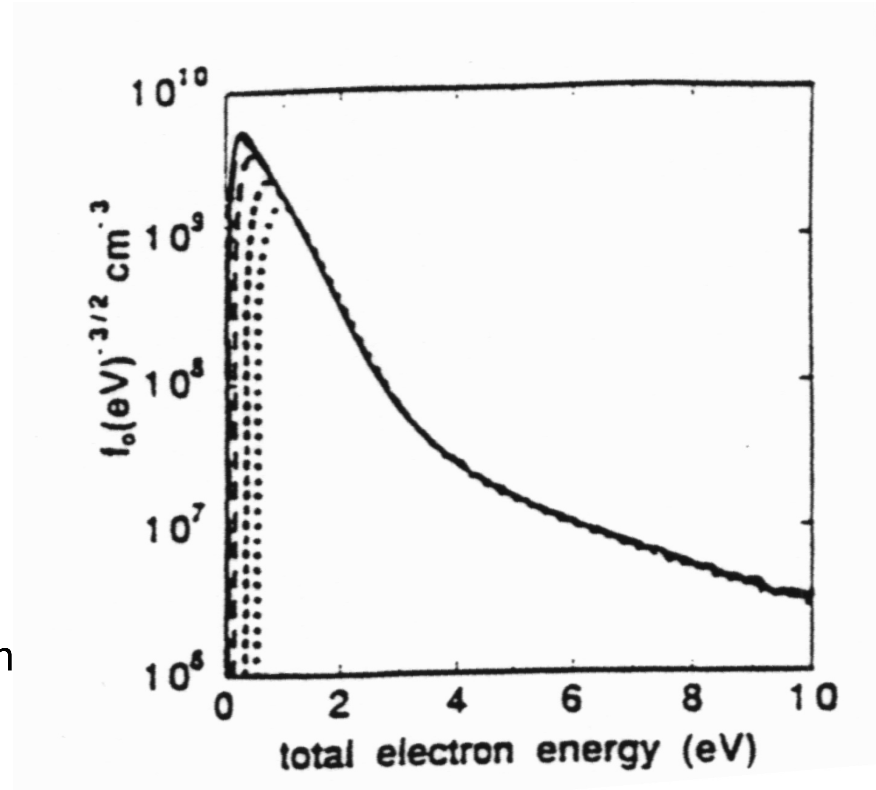

Experimental EEDF's at different positions

capacitively coupled RF discharge in argon 0.03 Torr, 13.56 MHz;

Exp.: V. A. Godyak and R. B. Piejak, APL 1993

PIC: V. A. Schweigert, *et al*, Appl. Phys. Lett. 69, 2341 (1996).

EXAMPLE: NONLOCAL ELECTRON KINETIC EFFECTS IN INDUCTIVE DISCHARGE

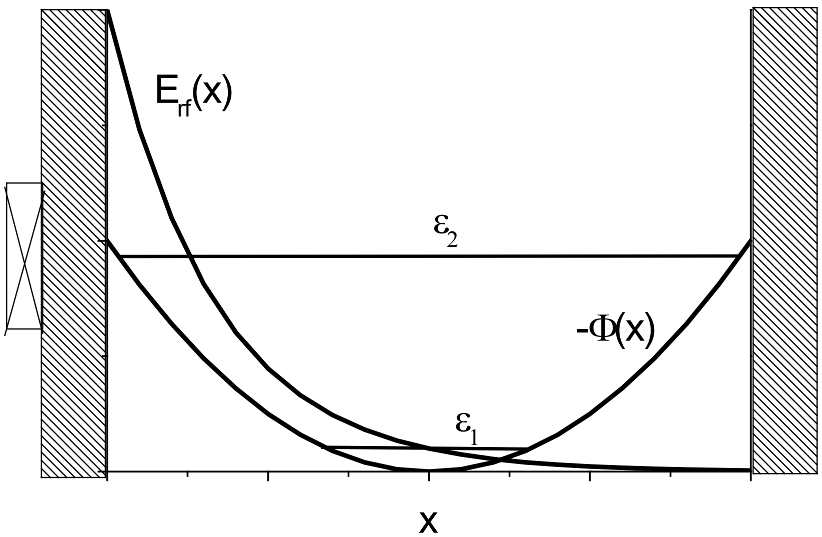

rf electric field

$$\frac{d^2E_y}{dx^2}+\frac{\omega^2}{c^2}E_y=-\frac{4\pi i\omega}{c^2}[j(x)+I\delta(x)]$$

$$J_y(x)=\frac{e^2n_{e0}}{m}\left(\int_0^x G(x,x')E_y(x')dx'+\int_x^L G(x',x)E_y(x')dx'\right)$$

$$-\frac{d}{d\varepsilon}(D_\varepsilon+\overline{D_{ee}})\frac{df_0}{d\varepsilon}-\frac{d}{d\varepsilon}\overline{V_{ee}}f_0=\sum_k\left[\overline{\nu_k^*(u+\varepsilon_k^*)\frac{\sqrt{(u+\varepsilon_k^*)}}{\sqrt{u}}f_0(\varepsilon+\varepsilon_k^*)}-\overline{\nu_k^*}f_0\right],$$

D_{ee} V_{ee} are from the electron-electron collision integral,
ν^* is inelastic collision frequency,
D_e is energy diffusion coefficient is a function of the rf electric field E_y and the plasma potential $\varphi(x)$.

upper bar denotes space averaging with constant total energy.

COMPARISON WITH EXPERIMENT $\frac{c}{\omega_{ep}} < \delta < \frac{V_{Te}}{\omega}$

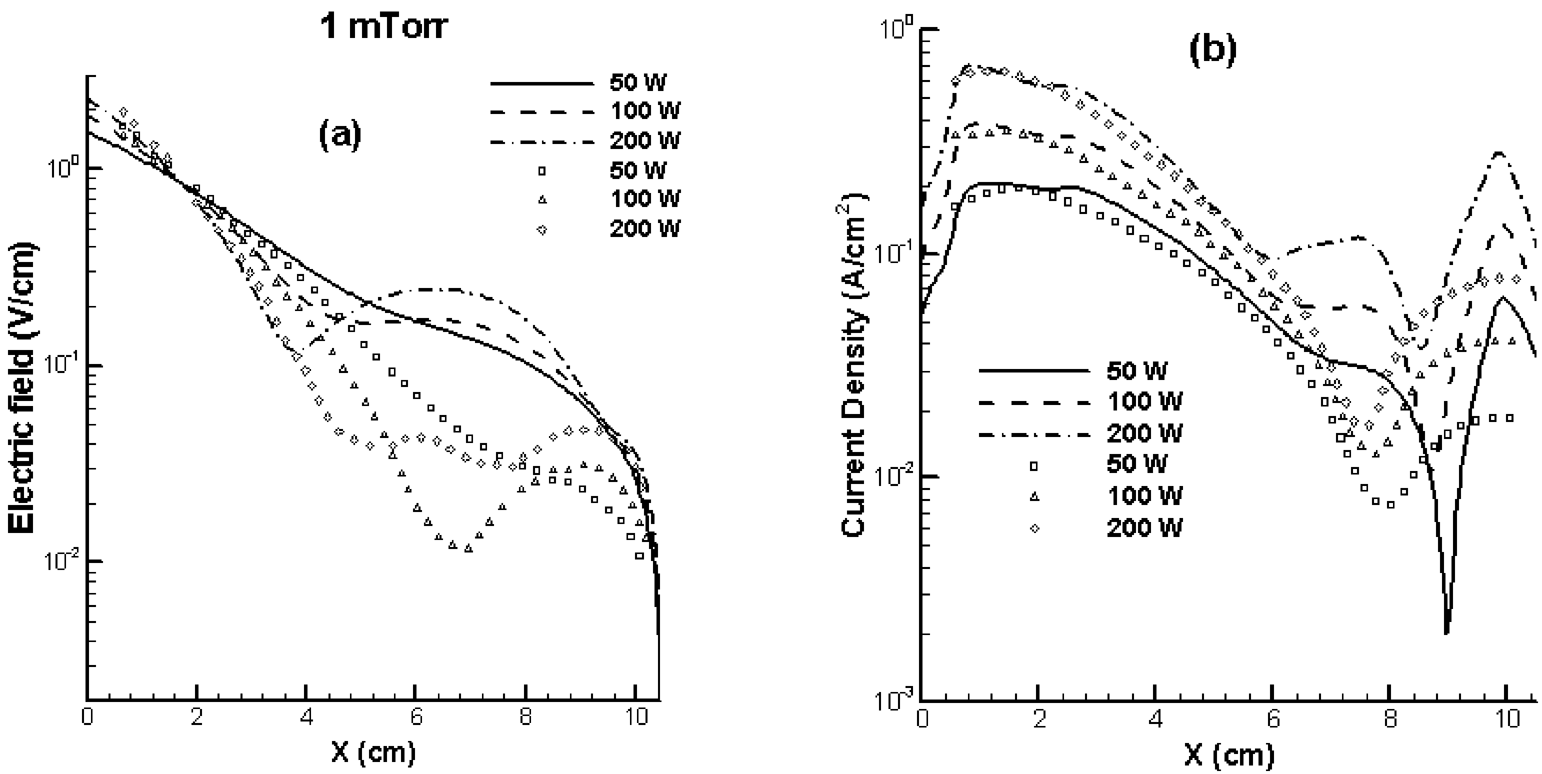

Experimental data (symbols) and simulation (lines)
(a) RF electric field and (b) the current density profiles for a argon pressure of 1 mTorr.

V. A. Godyak and R. B. Piejak, J. Appl. Phys. **82**, 5944 (1997).
B. Ramamurthi, *et al*, Plasma Sources Sci. Technol. **12**, 170 (2003).

Comparison With Experiment for ICP With External Magnetic Field

Experiment: V.A. Godyak and B. M. Alexandrovich, Phys. Plasmas **11**, 3553 (2004).
Simulations O. Polomarov *et al*, IEEE TPS **34**, 767 (2006).

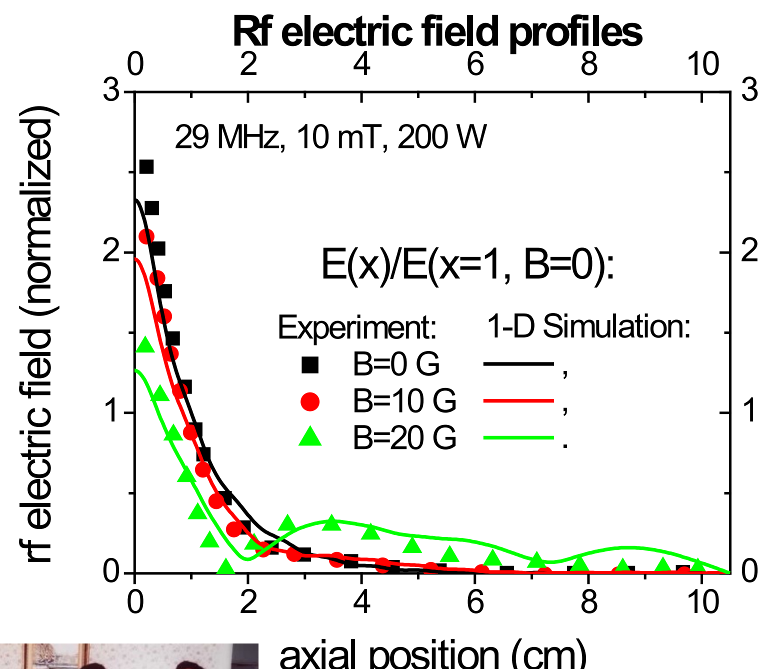

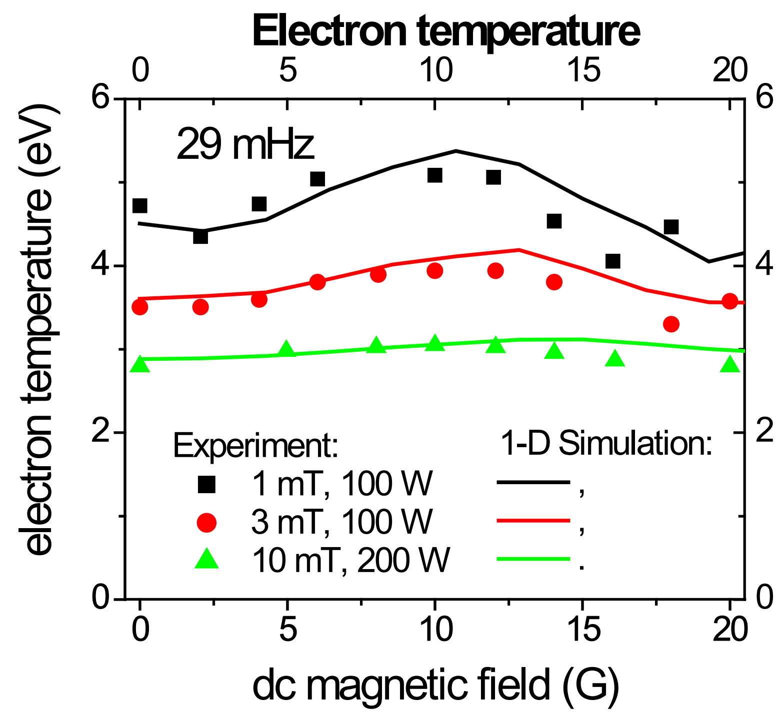

INFLUENCE OF PLASMA POTENTIAL ON RF HEATING

Surface impedance for different plasma profiles.

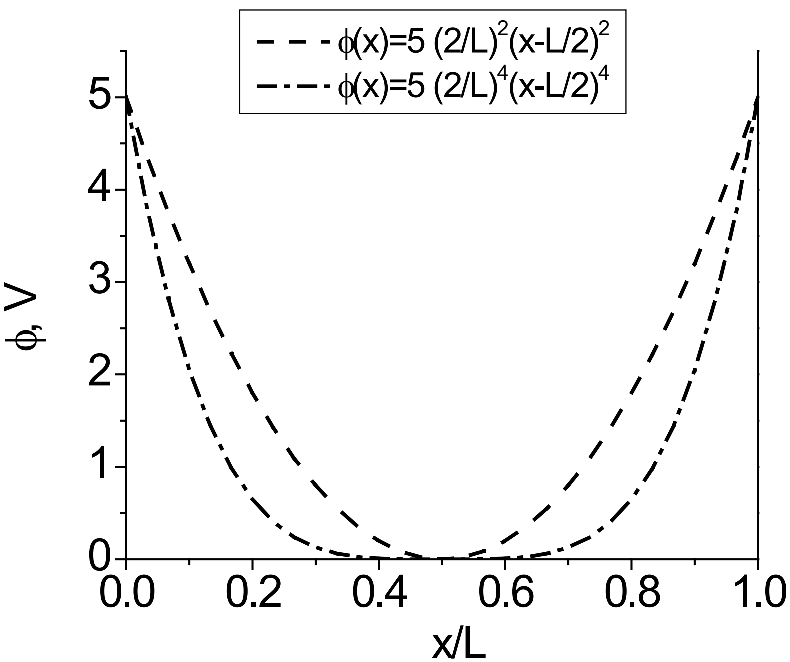

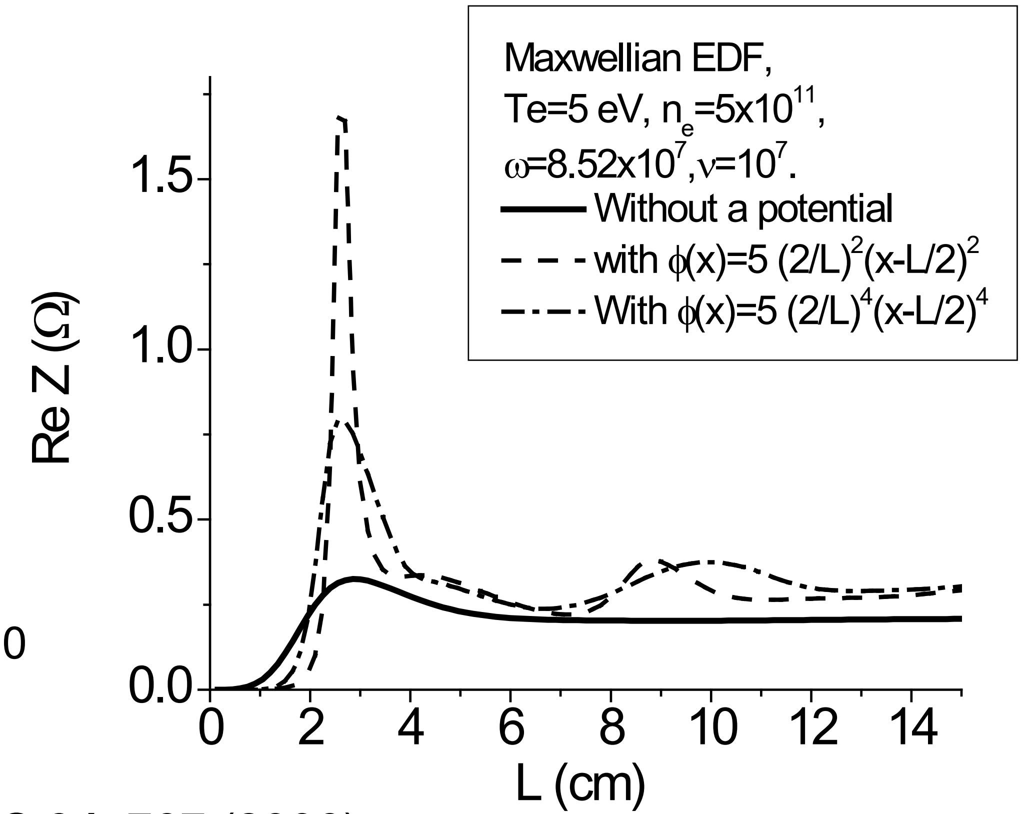

Theory: O. Polomarov *et al*, IEEE TPS **34**, 767 (2006).
Experiment: Chin Wook Chung et al, Phys. Plasmas **8**, 2992 (2001).

COMPARISON OF RESULTS OF BOUNCE-AVERAGED KINETIC EQUATION WITH EXPERIMENT

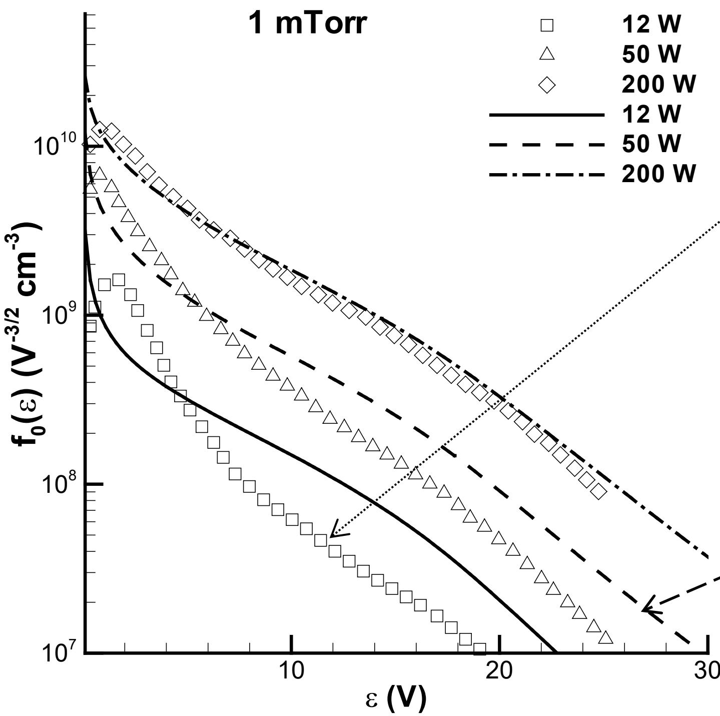

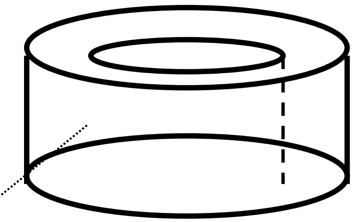

R=10cm,L=10cm, antenna R=4cm

$$\frac{\partial}{\partial\varepsilon}\left(D_\varepsilon(\varepsilon)\frac{\partial f_0}{\partial\varepsilon}\right)=\overline{S(f_0)},$$

where $D_\varepsilon(\varepsilon)$ is the energy diffusion coefficient given by

$$D_\varepsilon(\varepsilon)=\frac{\pi}{8}\left(\frac{2e}{m}\right)^{3/2}\sum_{n=-\infty}^{\infty}\int_0^{\varepsilon}\mathrm{d}\varepsilon_x|E_{yn}(\varepsilon_x)|^2(\varepsilon-\varepsilon_x)\times\frac{\nu}{\Omega_\mathrm{b}(\varepsilon_x)([\Omega_\mathrm{b}(\varepsilon_x)n-\omega]^2+\nu^2)}.$$

EEDF simulated (lines) and experimental data (symbols) for 1 mTorr.

V. A. Godyak and V. I. Kolobov, Phys. Rev. Lett., **81**, 369 (1998).

B. Ramamurthi, et al, Plasma Sources Sci. Technol. **12**, 302 (2003).

FROM METHODS TO CONTROL ELECTRON VELOCITY DISTRIBTUION FUNCTIONS TO PRACTICAL APPLICATIONS

METHODS OF CONTROL

- **Auxiliary biased electrodes**
- **Emission from the surface**
- **Hybrid DC/RF unmagnetized**
- **Magnetized plasma sources**
- **Injection of electron beam into the plasma**

APPLICATIONS

- **Non-ambipolar electron plasma.**
- **DC/RF Plasma Source for Plasma Processing**
- **Tokamak-wall cleaning**
- **Electric Propulsion**
- **High power plasma switch for electric grid system.**

CONTROLLING PLASMA PROPERTIES WITH APPLIED MAGNETIC FIELD

Applications: Electric Propulsion, Plasma Sources for Ion Beams, Magnetron Discharges, High Power Plasma Switch

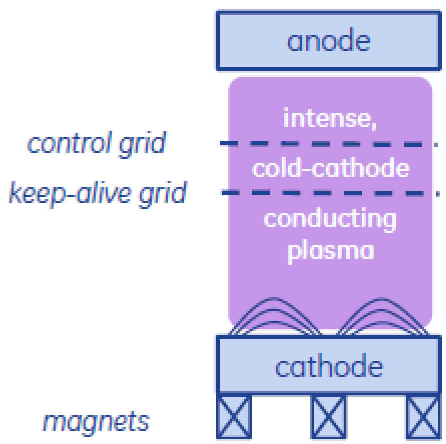

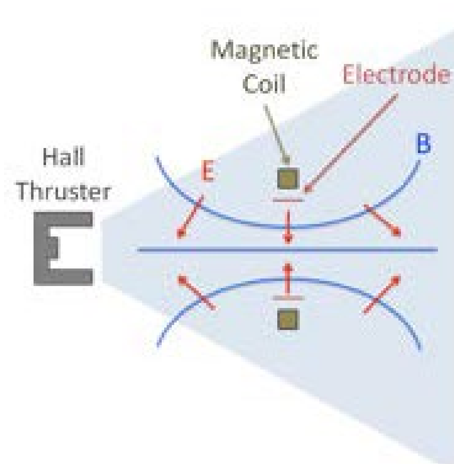

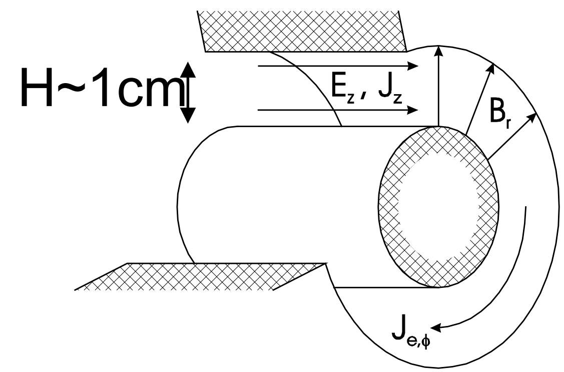

CONTROLLING PLASMA PROPERTIES IN LOW-COLLISIONAL PLASMAS WITH ACTIVE BOUNDARIES

Scope: The plasma-surface interaction in presence of strong thermionic or secondary electron emission has been studied theoretically and experimentally both as a basic phenomenon and in relation to numerous plasma applications such as, for example, cathodes, emissive probes, divertor plasma, surface discharges, dusty plasmas, plasma thrusters and plasma processing.

Main objective: To control plasma properties in systems having active boundaries, including biased, emissive and absorbing walls

Approach: We evaluate modifications of non-local electron kinetics and global properties of magnetized and non-magnetized plasmas by applying voltages to auxiliary electrodes and using emitting boundaries at different gas pressures

PPPL
PRINCETON
PLASMA PHYSICS
LABORATORY

UNIVERSITY OF ALBERTA

WestVirginiaUniversity

THE UNIVERSITY of WISCONSIN MADISON

PLASMA-WALL INTERACTIONS IN HALL THRUSTERS

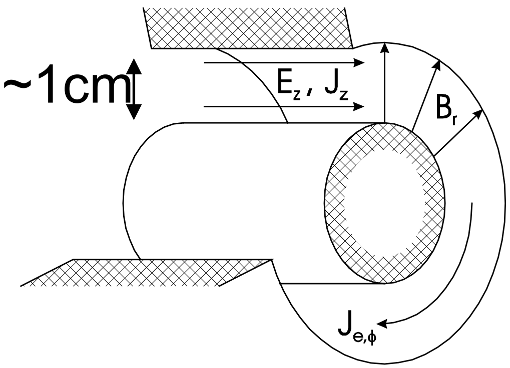

B ~ 100G, E ~ 100V/cm, T_e ~ 100eV. P=0.1-1mTorr, the plasma inside the thruster channel is collisionless, λ_{ec} (~1m) >> H (~1cm). => intense particle and heat wall losses!

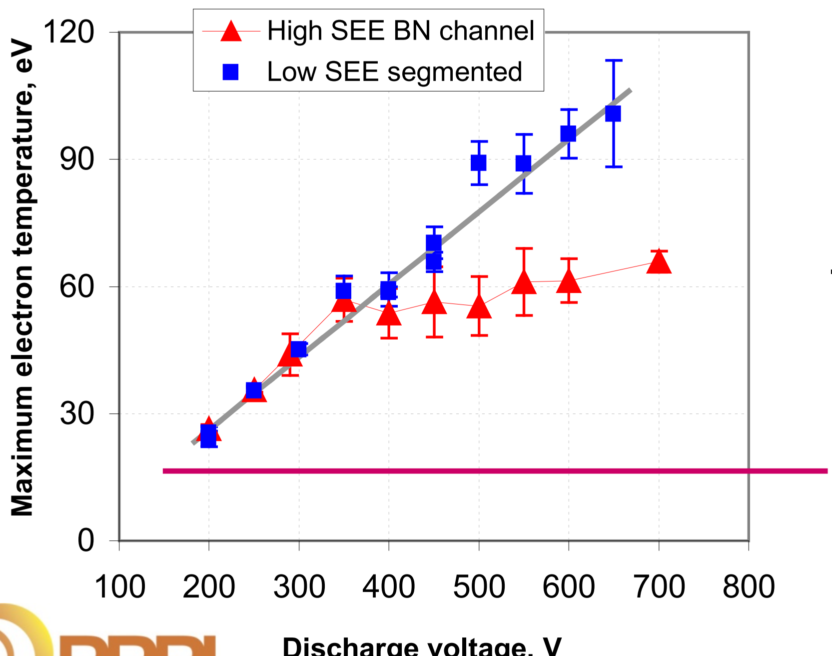

High electron temperature is observed in experiments

- ***Large quantitative disagreement with fluid theories.***

A fluid theory prediction.

From: Y. Raitses, *et al.*, Phys. Plasmas **13**, 014502 2006.

PRINCETON PLASMA PHYSICS LABORATORY

PARTICLE-IN-CELL SIMULATIONS OF HALL THRUSTER PLASMA

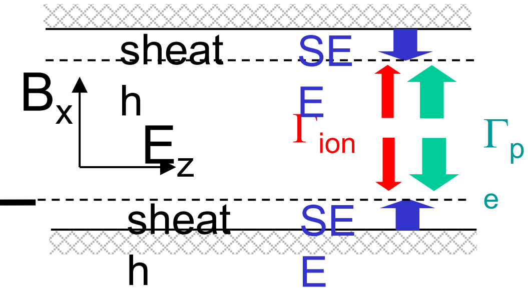

Complex structure of strongly anisotropic (T_x = 12eV, T_z = 37eV!) electron velocity distribution function (EVDF) in the channel of a Hall thruster discharge (left) versus an isotropic Maxwellian EVDF (right).

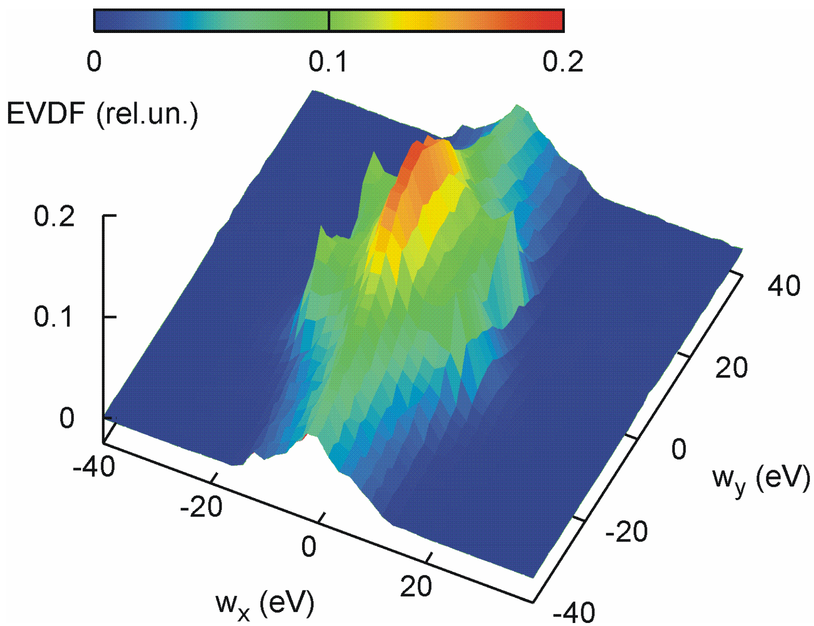

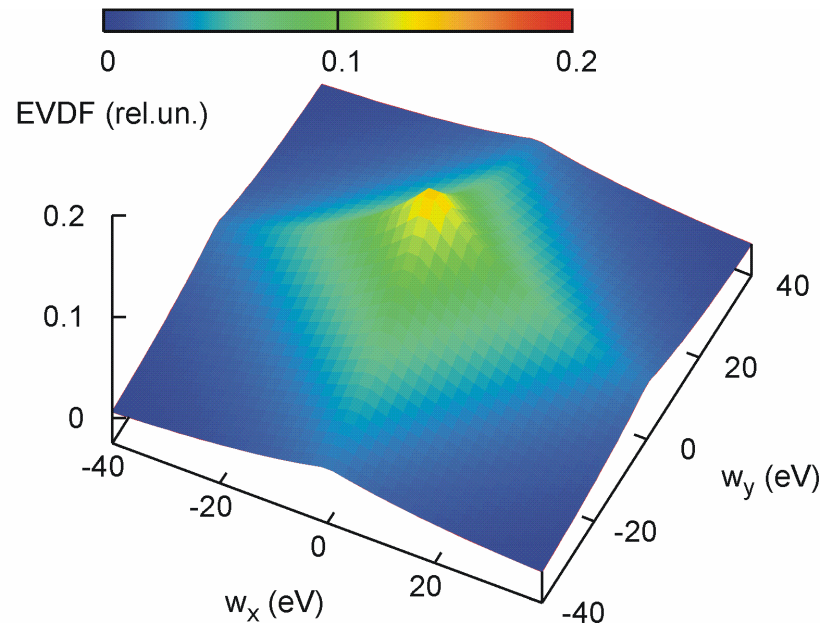

=> Completely different implications follow from kinetic or fluid description for the Hall thruster operation.

PPPL PRINCETON PLASMA PHYSICS LABORATORY

UNIVERSITY OF ALBERTA

CONTROLLING PLASMA PROPERTIES: ELECTRON INDUCED SECONDARY ELECTRON EMISSION

- Kinetic studies of bounded plasmas by walls having secondary electron emission (SEE) predict a strong dependence of wall potential on SEE [1-4].
- Sheath oscillations occur due to coupling of the sheath potential and non-Maxwellian electron energy distribution functions [1,2].

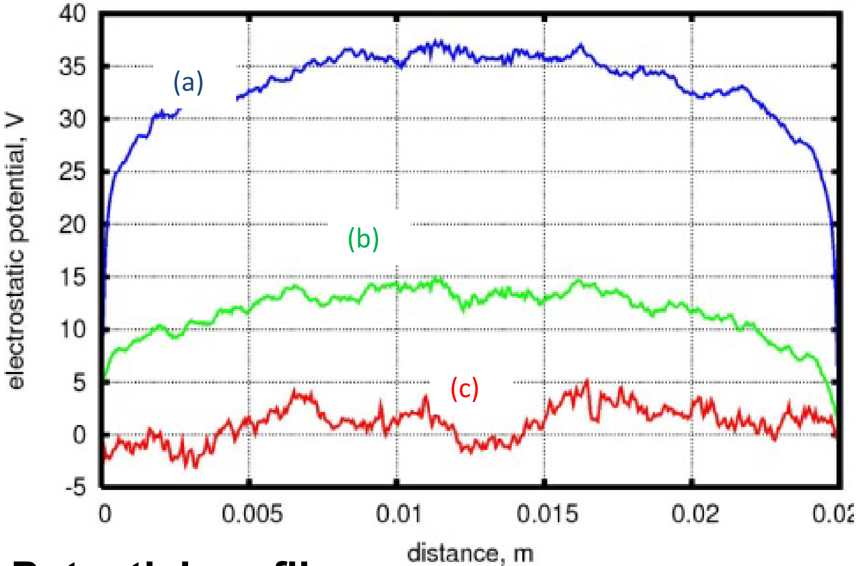

Potential profiles:
(a) E=200V/cm no emission
(b) E=200V/cm with SEE,
(c) E =250V/cm with SEE [1,3]

- When electrons impacting walls produce more than one secondary on average no classical sheath exists.
- Strong dependence of wall potential on SEE allows for active control of plasma properties by judicious choice of the wall material.

[1] Phys. Rev. Lett. 103, 145004 (2009)
[2] Phys. Rev. Lett. 108, 235001 (2012)
[3] Phys. Rev. Lett. 108, 255001 (2012)
[4] Phys. Plasmas 19, 123513 (2012)

PRINCETON PLASMA PHYSICS LABORATORY
UNIVERSITY OF ALBERTA

THREE PARTICLE-IN-CELL CODES HAVE BEEN UTILIZED FOR THEORETICAL STUDIES

- **An electrostatic parallel, implicit, 2D PIC code EDIPIC. Implemented electron-atom scattering, ionization, and excitation as well as electron-ion and electron-electron collisions.**

- **3D LSP code includes electromagnetic and electrostatic modules. In collaboration with Voss Scientific.**

- **Novosibirsk group PIC code, 2D-3D PIC code with numerical acceleration schemes using fluid closures**

PPPL
PRINCETON
PLASMA PHYSICS
LABORATORY

UNIVERSITY OF ALBERTA

ИТПМ

Numerical Methods

	Pros	Cons
PARTICLE-IN-CELL CODES	Easy algorithms. Easy implementation Easy 3D implementation	Numerical noise Limitations on Debye Radius
Direct Vlasov Solvers + Discontinuous Galerkin	Possibly can avoid limitations on Debye Radius Low numerical noise	Numerical diffusion Positive f requirement Complex 3D implementation
Hybrid: fluid + MC for fast particles	Possibly can avoid limitations on Debye Radius Low numerical noise	Cannot describe collective and kinetic processes

Preferred Computational Tool - PIC

Parallel, implicit particle-in-cell code with energy corrections and noise control is a powerful and versatile tool.

- Ease of coding
- Modular, “easy” for parallelization
- Modern clusters and multi cores PCs are cheap

3D code for Plasma Panel Modeling

Up to 250 million of ions and electrons on up to 64 processors, up to 150x150x150 meshes

V. N. Khudik, A. Shvydky, V. P. Nagorny, and C.E. Theodosiou, *IEEE Trans Plasma Sci.* **33**, 510 (2005).

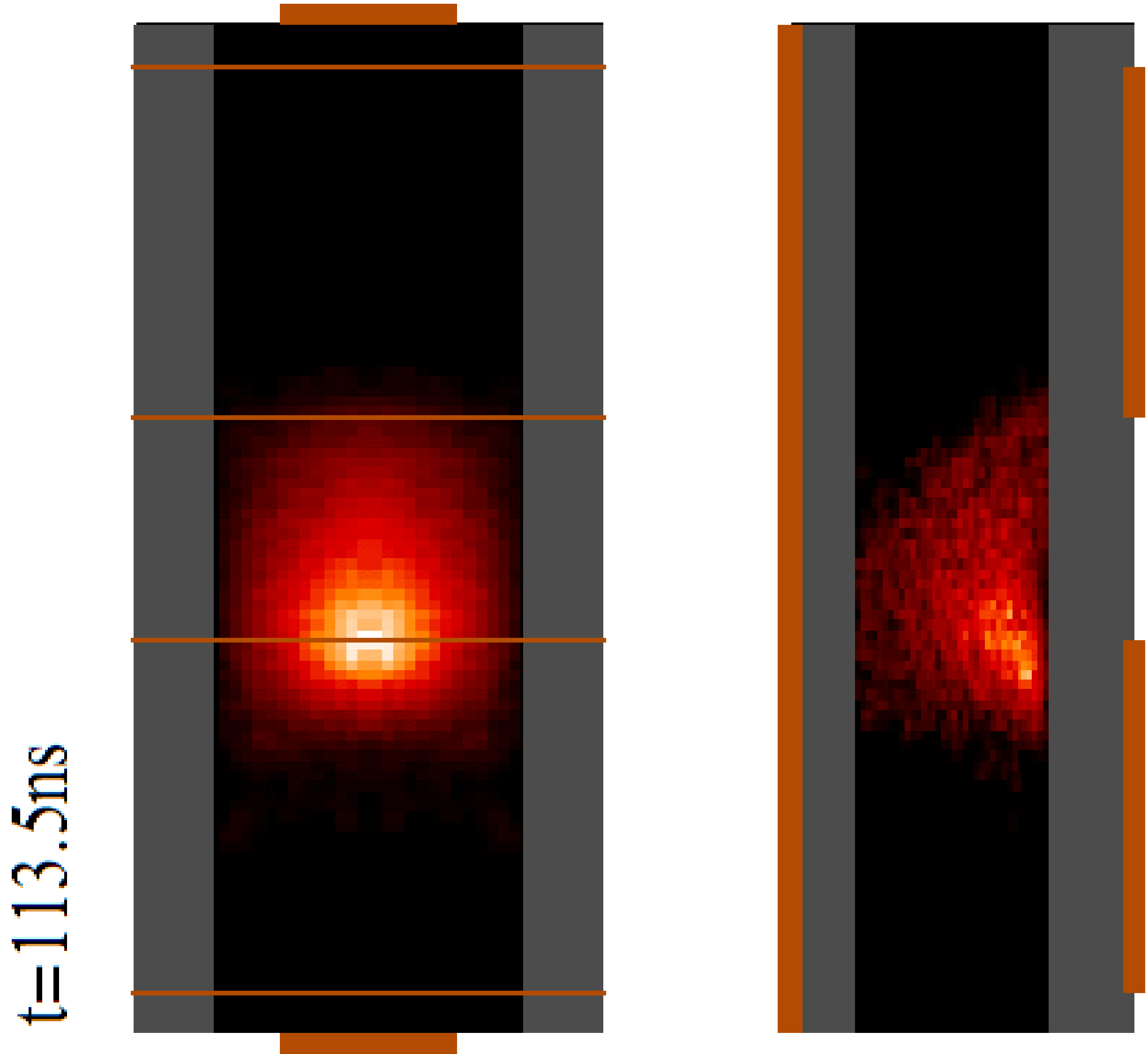

PDP discharge phases

experiment

PIC simulations

Top view

Side view

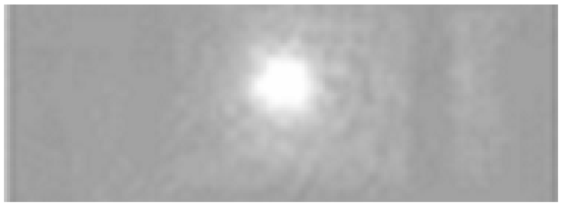

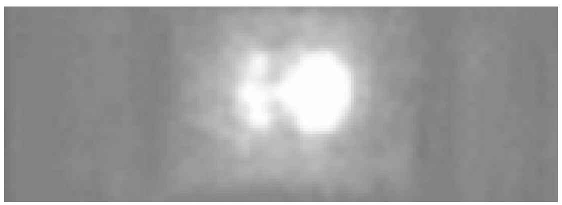

V. N. Khudik, A. Shvydky, V. P. Nagorny, and C.E. Theodosiou, *IEEE Trans Plasma Sci.* **33**, 510 (2005).

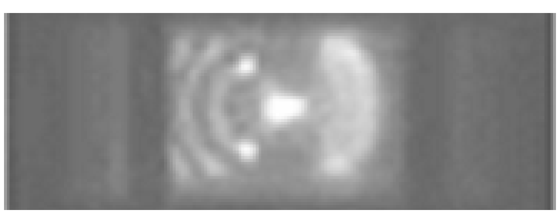

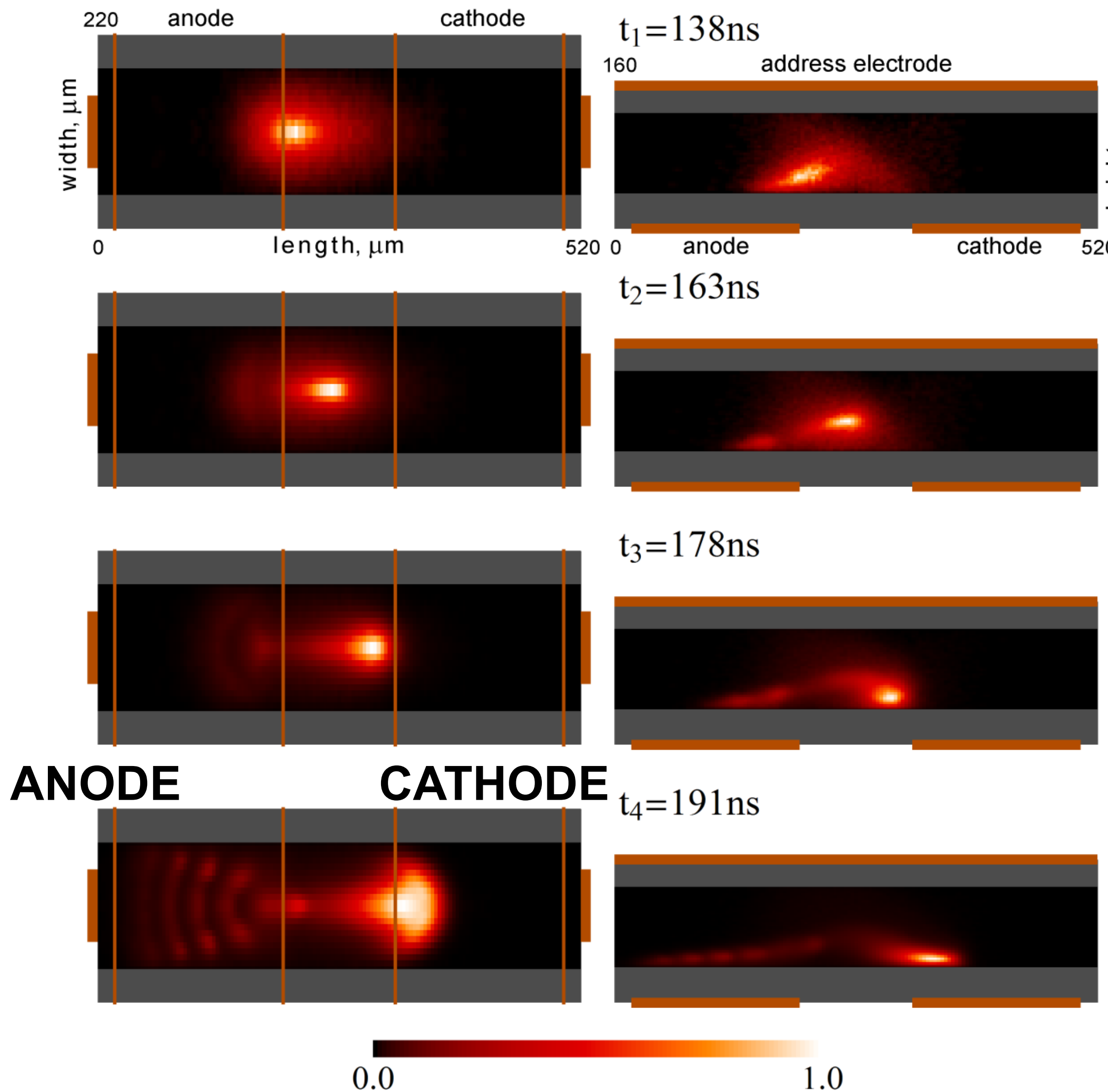

CONTROLLING PLASMA PROPERTIES BY MANAGING FAST ELECTRONS WITH AUXILIARY ELECTRODES

Changing voltage on diaphragm electrode leads to transitions between two very different discharge modes.

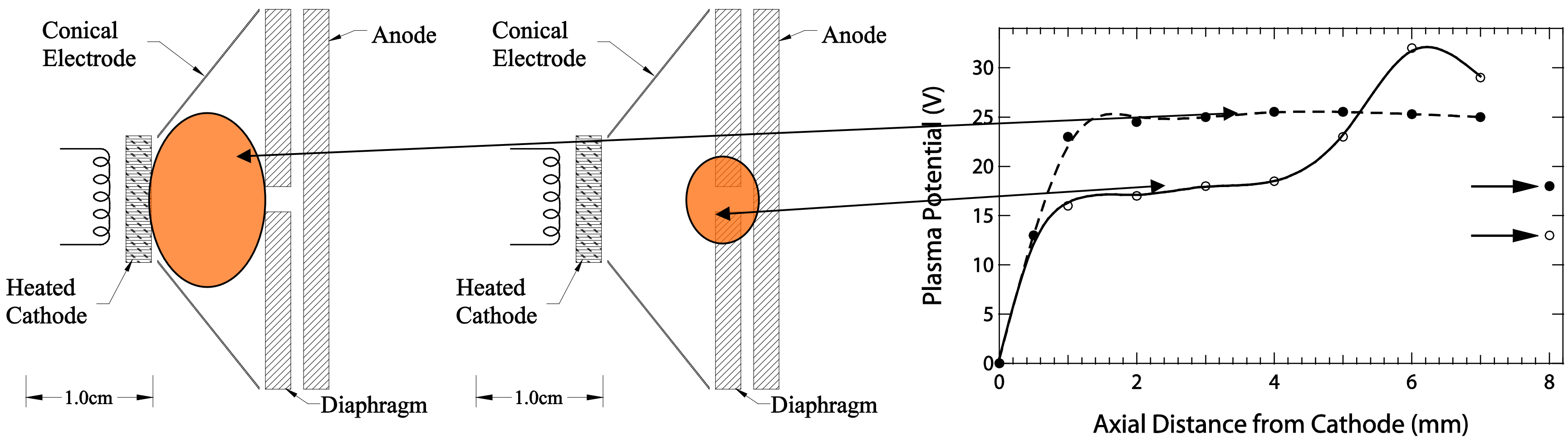

Left: Schematic diagram of the experimental device of dc discharge with hot cathode and plasma glow, He 1 Torr.
Right: Axial profiles of the plasma potential for voltages on diaphragm 18V and 13V.

CONTROLLING PLASMA PROPERTIES BY MANAGING FAST ELECTRONS WITH AUXILIARY ELECTRODES

Formation of nonmotonic EEDF with enhanced group of fast electrons in the diaphragm tunnel.

j_{an} =0.1 A, 1Torr and U_d = 11 V.

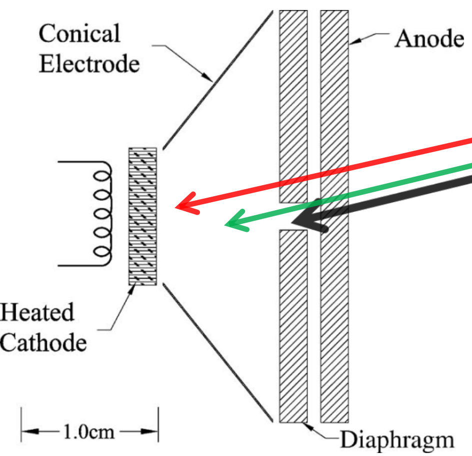

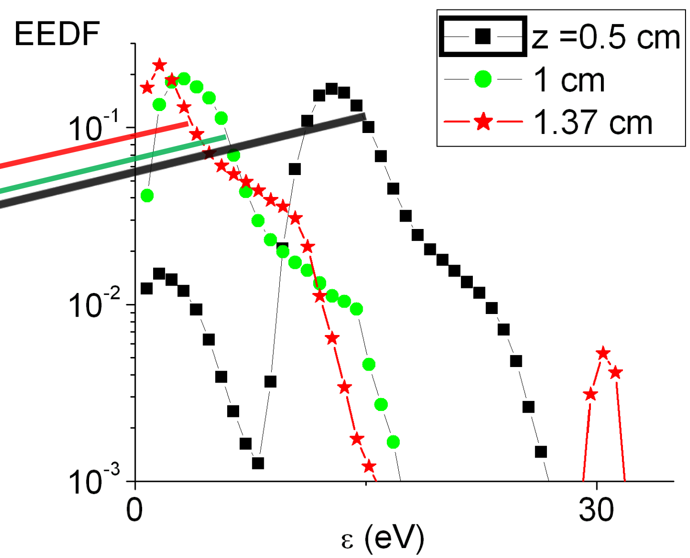

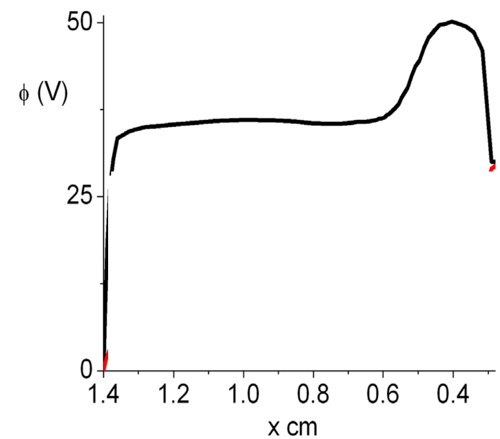

I.V. Schweigert, I. D. Kaganovich, and V. I. Demidov, "Active electron energy distribution function control in dc discharge using an auxiliary electrode" ;
E. Bogdanov, V. I. Demidov, I. D. Kaganovich, A. A. Kudryavtsev, S. F. Adams, and M. E. Koepke, "Modeling a short dc discharge with thermionic cathode and auxiliary anode for suppression of discharge oscillations" accepted Phys. Plasmas (2013).

OUTLINE

- Motivation
- Brief Summary of Research in Low Temperature Plasma Physics at PPPL
- Description of Codes
- **Beam-plasma interaction in a bounded plasma (two-stream instability):**
  - Effects of finite size and boundaries
  - Effects of nonuniform plasma
  - Mechanism of electron acceleration in plasma wave

PPPL
PRINCETON PLASMA PHYSICS LABORATORY

CONTROLLING PLASMA PROPERTIES BY INEJCTION OF ELECTRON BEAM INTO THE PLASMA

Applications: Plasma Processing Systems, Gas Lasers, Ionization at High Pressures

Electron beam generated plasma processing system

Large Area Plasma Processing System (LAPPS)*

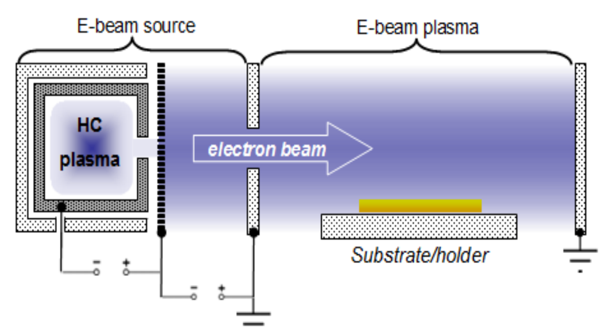

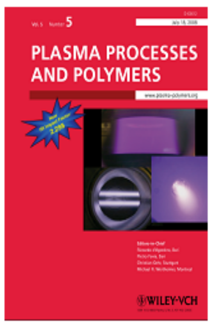

S.G. Walton *et al*, Plasma Proc. and Poly. 5, 453 (2008)

Basic Operation for Processing System

- High-energy (few keV), sheet beam injected into background
- Magnetically collimated to minimize spreading
- Creates plasma sheet parallel to substrate surface
- Large amount of flexibility in system design

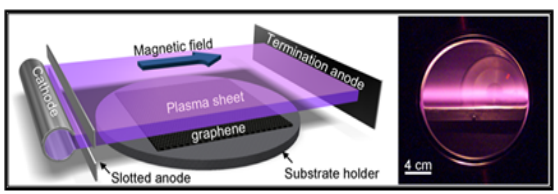

M. Baraket *et al*, App. Phys. Lett. 100, 233123 (2012)

* Meger et al., US patent no. 5,874,807 (Feb. 1999)

PRINCETON PLASMA PHYSICS LABORATORY

Collisionless Electron Beam Interaction with Background Plasma

Electron beam emitted from the walls can interact with plasma and effectively transfer energy to background electrons and ions.

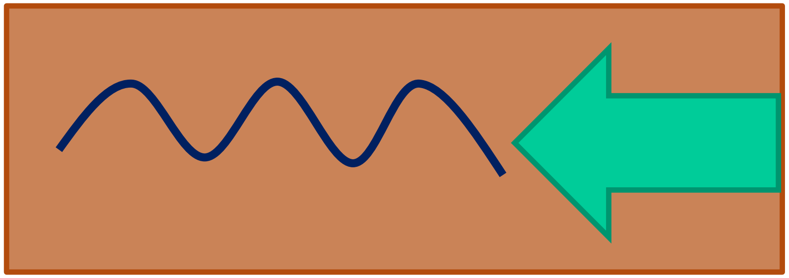

Questions:

How effective is this process?
What are resulting electron and ion energy distribution functions?

HYBRID RF-DC PLASMA SOURCES PROVIDE DIRECT E-BEAM SURFACE INTERACTIONS

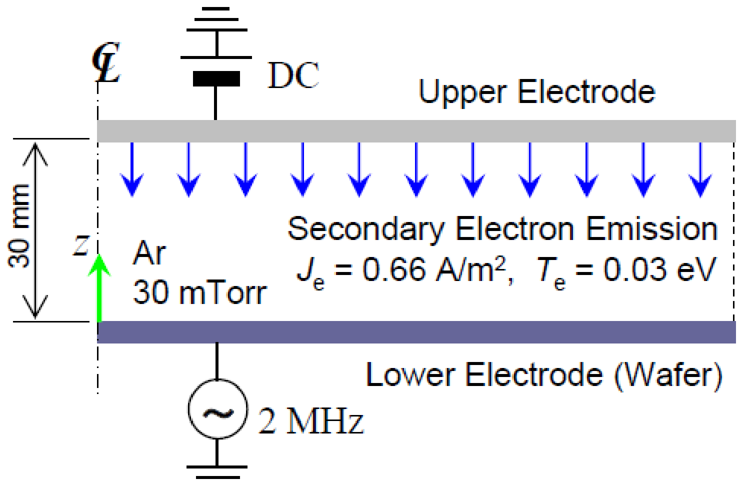

DC-RF system yielded increased film etch rate, but reduced photoresist etch rate.
e-beam→ surface or bulk plasma chemistry effect?

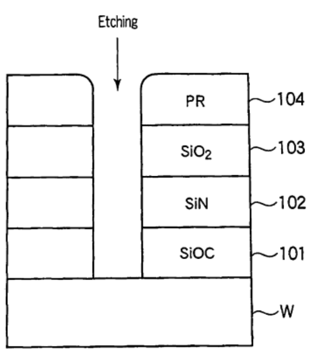

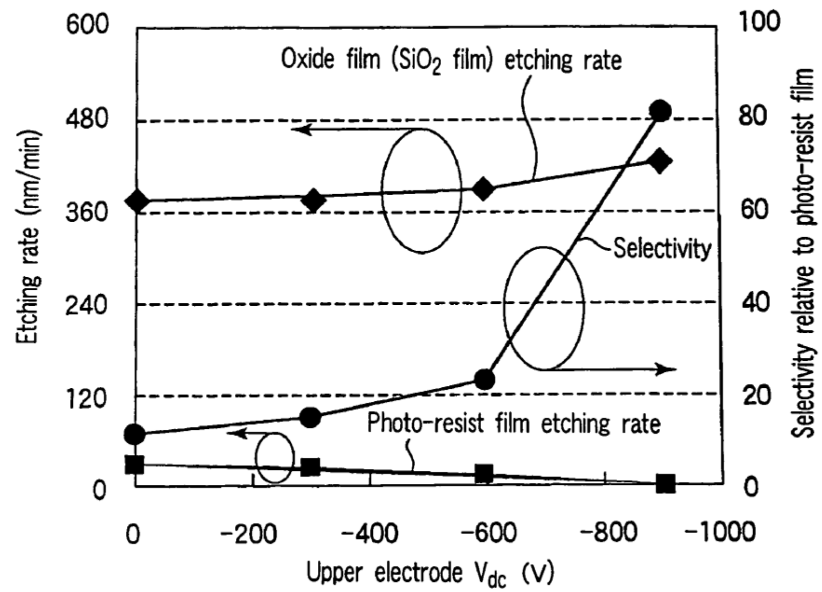

Koshiishi '05

Courtesy of P. L. G. Ventzek

TOKYO ELECTRON

OBSERVATION OF MULTI-PEAK ELECTRON VELOCITY DISTRIBUTION FUNCTION

In experiments, Xu et al., APL 93 (2008) reproducible structures were observed in electron energy distributions at the RF electrode.

We performed large scaled simulations of this system millions of particles: 1000 spatial cells, 1000s particle per cell, time-averaging diagnostics for fine EVDF velocity and spatial resolution.

Observed excitation of plasma waves by the beam, then excitation of ion acoustic waves and intermittency of plasma turbulence. The electric field in plasma waves may be strong enough (~1kV/cm) to cause substantial direct plasma electron acceleration.

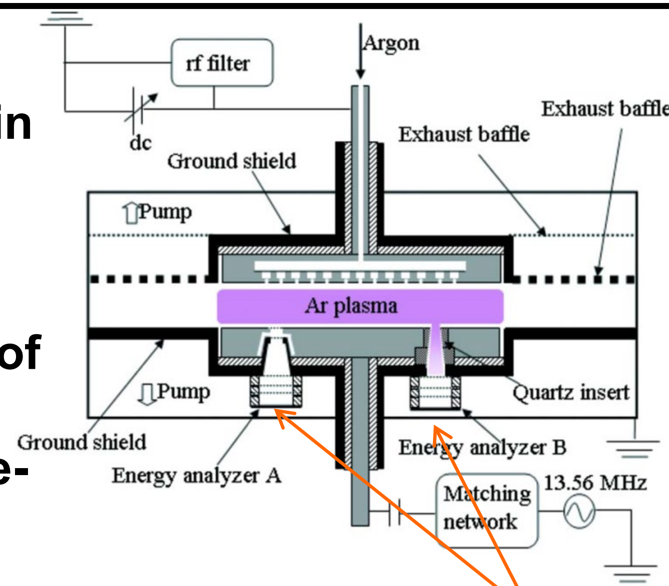

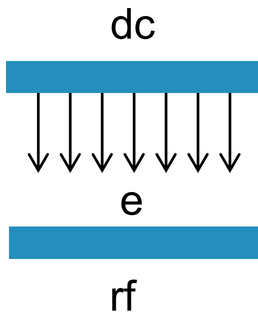

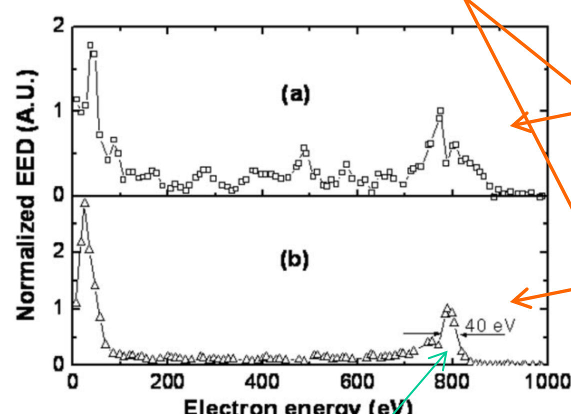

Energy analyzer A

Energy analyzer B

Beam energy is given by the DC potential, 800V

EDIPIC Code and Schematic of the Simulated System

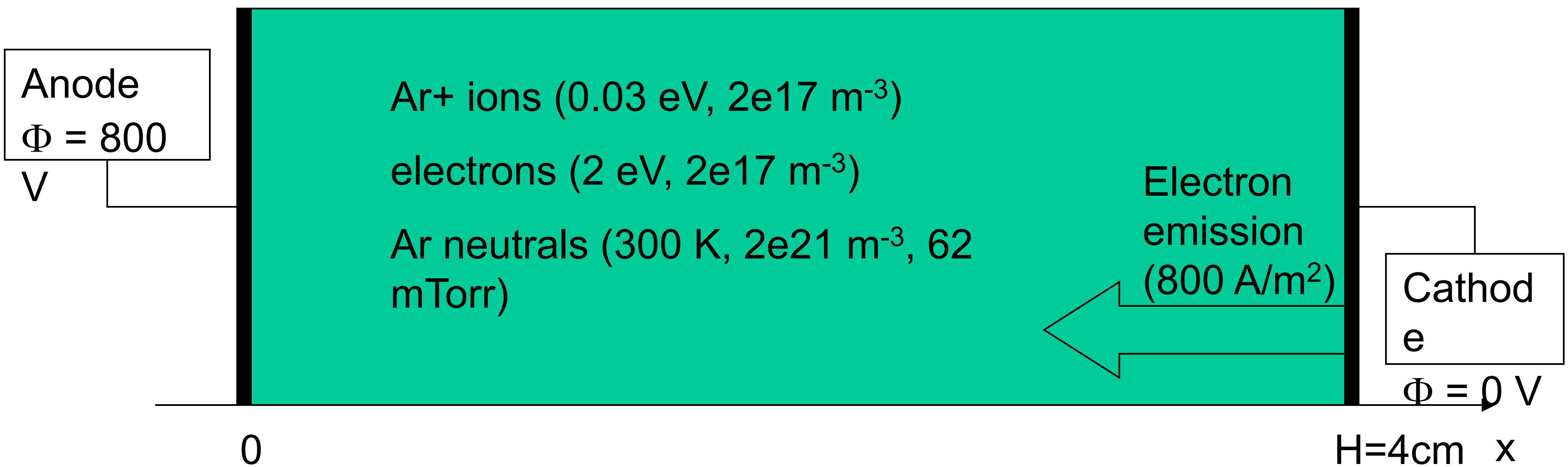

- EDIPIC- 1d3v parallel particle-in-cell code [*Sydorenko et al.,* 2006]:
  - direct implicit algorithm [*Gibbons and Hewett*, 1995]
  - Monte-Carlo collisions between electrons and neutrals
  - Electron-electron and electron-ion collisions
  - active material surfaces with secondary electron emission induced by incident electrons and ions
  - (10^7 particles, 1000 spatial cells, 1000s particle per cell, time-averaging diagnostics for fine EVDF velocity and spatial resolution)

Pierce Model (1944)

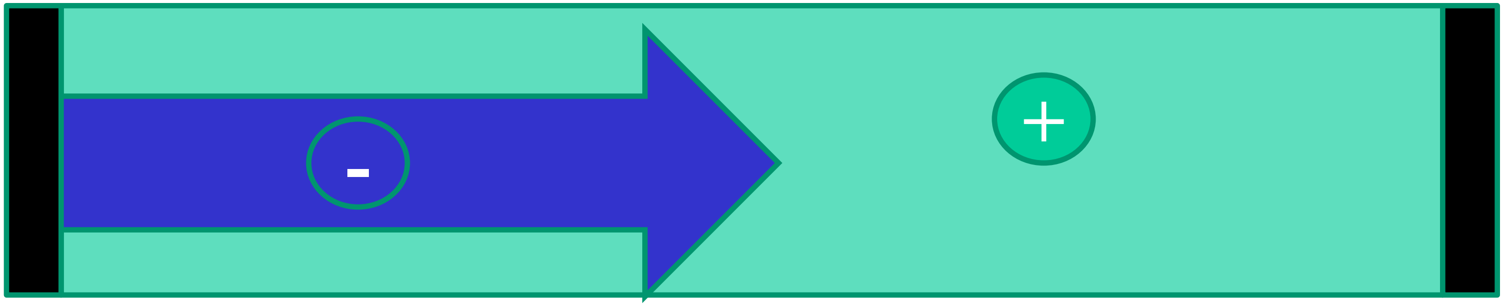

Electron beam is injected into ion background of equal density to the electron beam.

Electrodes with fixed potential set potential at boundaries.

Instability develops if $\omega_{pb} L / v_b > \pi$

This limits the current propagation through the gap.

Our Model (2015?)

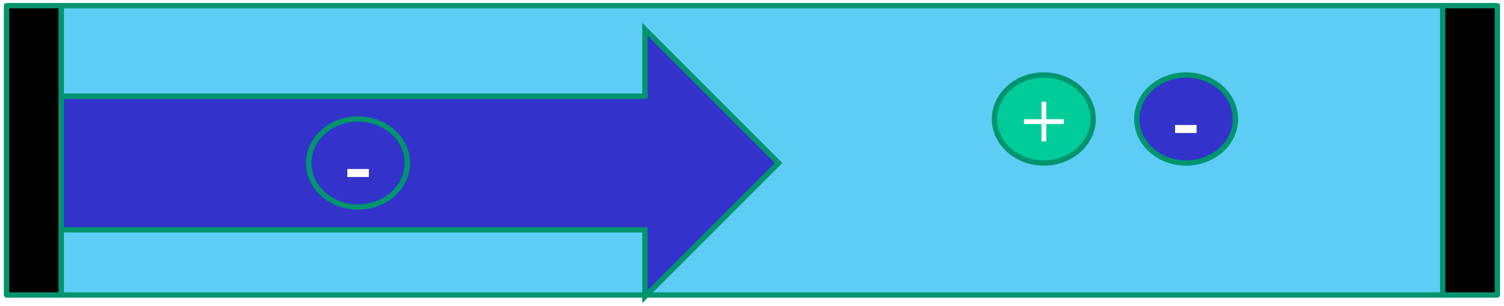

Electron beam is injected into electron and ion background of equal density.

Electrodes with fixed potential set potential at boundaries.

Instability is very different from textbook calculation for periodic b.c. $\omega_{e,0}\left(n_{b,0}/n_{e,0}\right)^{1/3}$

Analytic Solution

$$\frac{\partial n_{e,b}}{\partial t} + \frac{\partial v_{e,b} n_{e,b}}{\partial x} = 0$$

$$\frac{\partial v_{e,b}}{\partial t} + v_{e,b}\frac{\partial v_{e,b}}{\partial x} = -\frac{e}{m}E$$

$$\delta n_b(0) = \delta v_b(0) =$$

$$\delta\phi(0) = \delta\phi(L) = 0$$

$$\delta\phi(t,x) = \left(Ax + Be^{ik_+x} + Ce^{ik_-x} + D\right)e^{-i\omega t},$$

the following additional relation between ω and k:

$$k_-^2\left(e^{ik_+L} - 1\right) - \frac{ik_-^2 k_+ \omega L}{\omega - k_+ v_{b,0}} =$$

$$k_+^2\left(e^{ik_-L} - 1\right) - \frac{ik_+^2 k_- \omega L}{\omega - k_- v_{b,0}}. \qquad (10)$$

$$k_\pm = (1 \mp \chi)\frac{\omega_{e,0}}{v_{b,0}}$$

$$\Rightarrow \quad -i\frac{2(1-\chi)}{(1+\chi)\chi}L_n + e^{i(1-\chi)L_n} - 1-$$

$$\frac{(1-\chi)^2}{(1+\chi)^2}\left[e^{i(1+\chi)L_n} - 1\right] = 0$$

BANDWIDTH STRUCTURE OF GROWTH RATE OF TWO-STREAM INSTABILITY OF AN ELECTRON BEAM PROPAGATING IN A BOUNDED PLASMA

- **An analytical model of two-stream instability development,**
- **I. Kaganovich and D. Sydorenko (2015)**

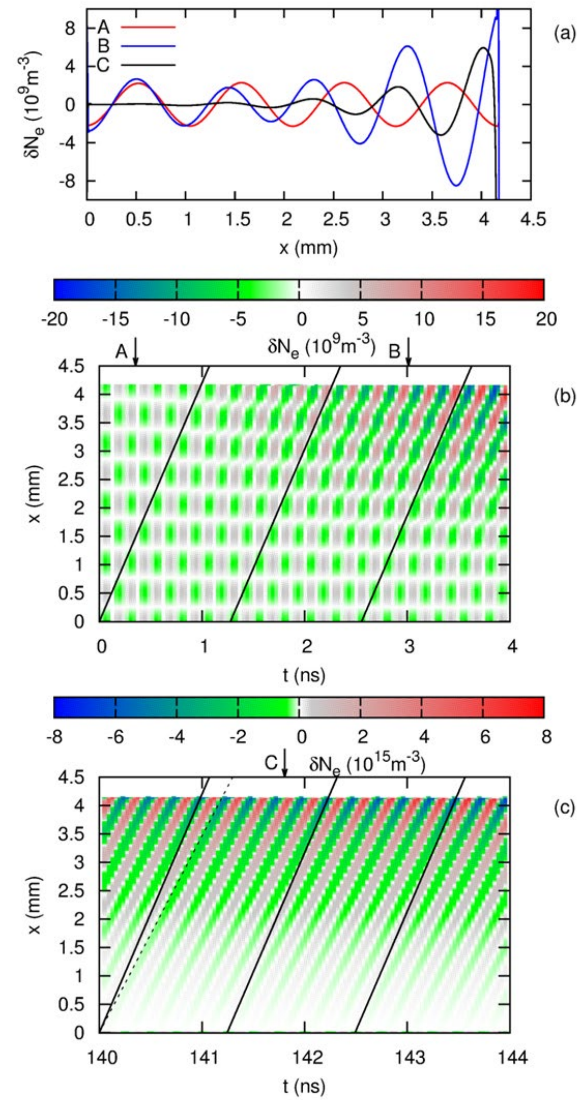

Fig. Dynamics of two-stream instability, the beam to plasma density ration, = 0.0006.

(a) Spatial profiles of bulk electron density perturbation obtained at t=0.35ns (curve A, red), t=3.01ns (curve B, blue), and t =141.8ns (curve C, black).

Panels (b) and (c) are color maps of evolution of density perturbations of bulk electron density in time intervals (b) 1-4ns, (c) 140-144ns. Here, solid black straight lines represent propagation with unperturbed beam velocity; dashed straight line represents phase velocity of the wave.

Comparison of analytic theory and PIC simulations

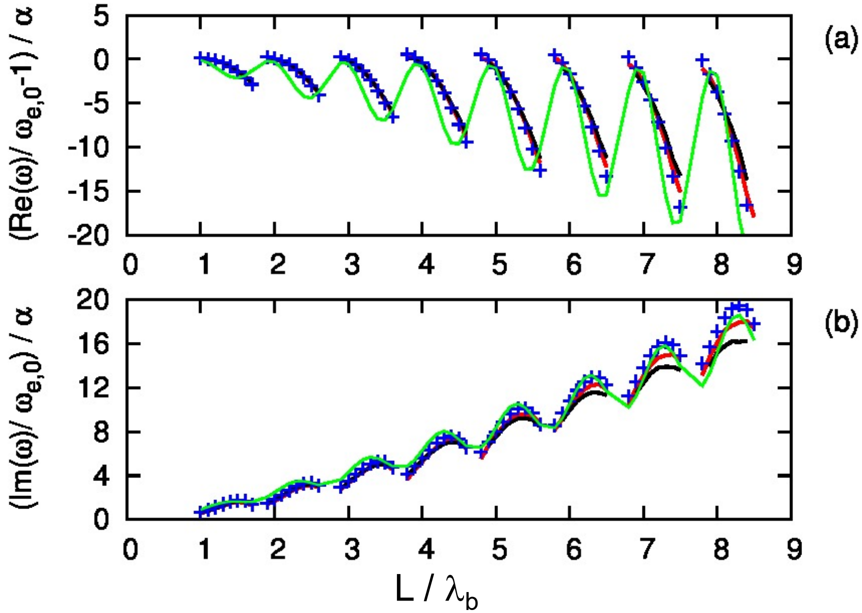

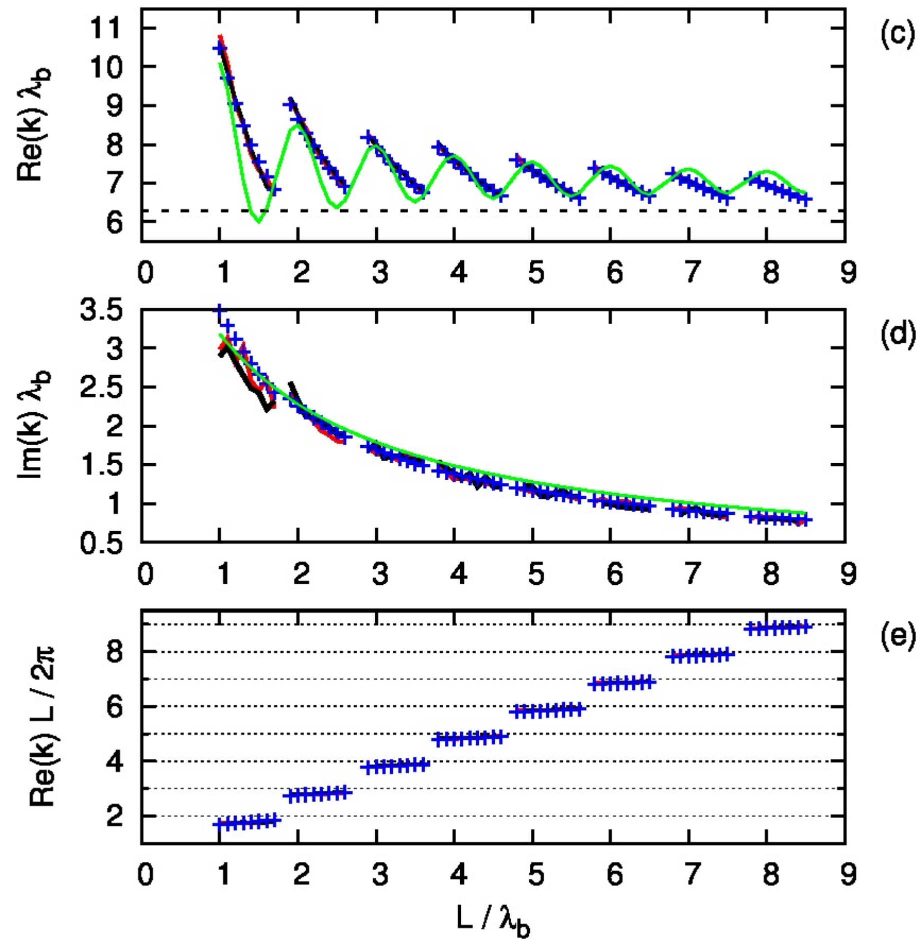

Frequency (a), temporal growth rate (b), wavenumber (c), spatial growth rate (d), and the number of wave periods per system length (e) versus the length of the system.
The blue crosses mark values obtained by analytical solution.

Solid red and black curves represent values obtained in fluid simulations with α = 0.00015 (red) and 0.0006 (black). Solid green curves are values provided by fitting formulas. In (c), the black dashed line marks the resonant wavenumber.

Summary of analytic model

We have studied the development of the two-stream instability in a finite size plasma bounded by electrodes both analytically and making use of fluid and particle-in-cell simulations.

We show that the instability reaches the asymptotic state when the wave structure has the same spatial profile and grows in time with a constant growth rate.

The spatial structure of the wave is close to a standing wave but has a spatial growth along the beam propagation.

We derived analytic expressions for the frequency, wave number and the spatial and temporal growth rates. Obtained analytic solution agrees well with the values given by fluid and particle-in-cell simulations.

- **Instability parameters are very different from the classical ones:**

growth rate $\boxed{Im(\omega) \approx \frac{1}{13} L_n \ln(L_n)\left[1 - 0.18\cos\left(L_n + \frac{\pi}{2}\right)\right]\alpha\omega_{pe},}$

where $L_n = L\omega_{pe}/v_b$, wavenumber $Re(k) \approx \frac{\omega_{pe}}{v_b}\left[1.1 + \frac{1+2.5\cos(L_n)}{1.1L_n}\right]$.

- **For comparison, the classical values:**

growth rate $Im(\omega) = 0.7\alpha^{1/3}\omega_{pe}$,

real resonance wavenumber $k = \omega_{pe}/v_b$.

OUTLINE

- **Beam-plasma interaction in a bounded plasma (two-stream instability):**
  - **Effects of finite size and boundaries:**
  - **Effects of nonuniform plasma**
    - **Density gradient plays a very important role in wave transformation and acceleration of bulk electrons.**
    - **It allows to couple the 800 eV beam and the bulk electrons with 2 eV temperature. =>**
  - **Mechanism of electron acceleration in plasma wave**

PRINCETON
PLASMA PHYSICS
LABORATORY

SIMULATION OF MULTI-PEAK ELECTRON VELOCITY DISTRIBUTION FUNCTION

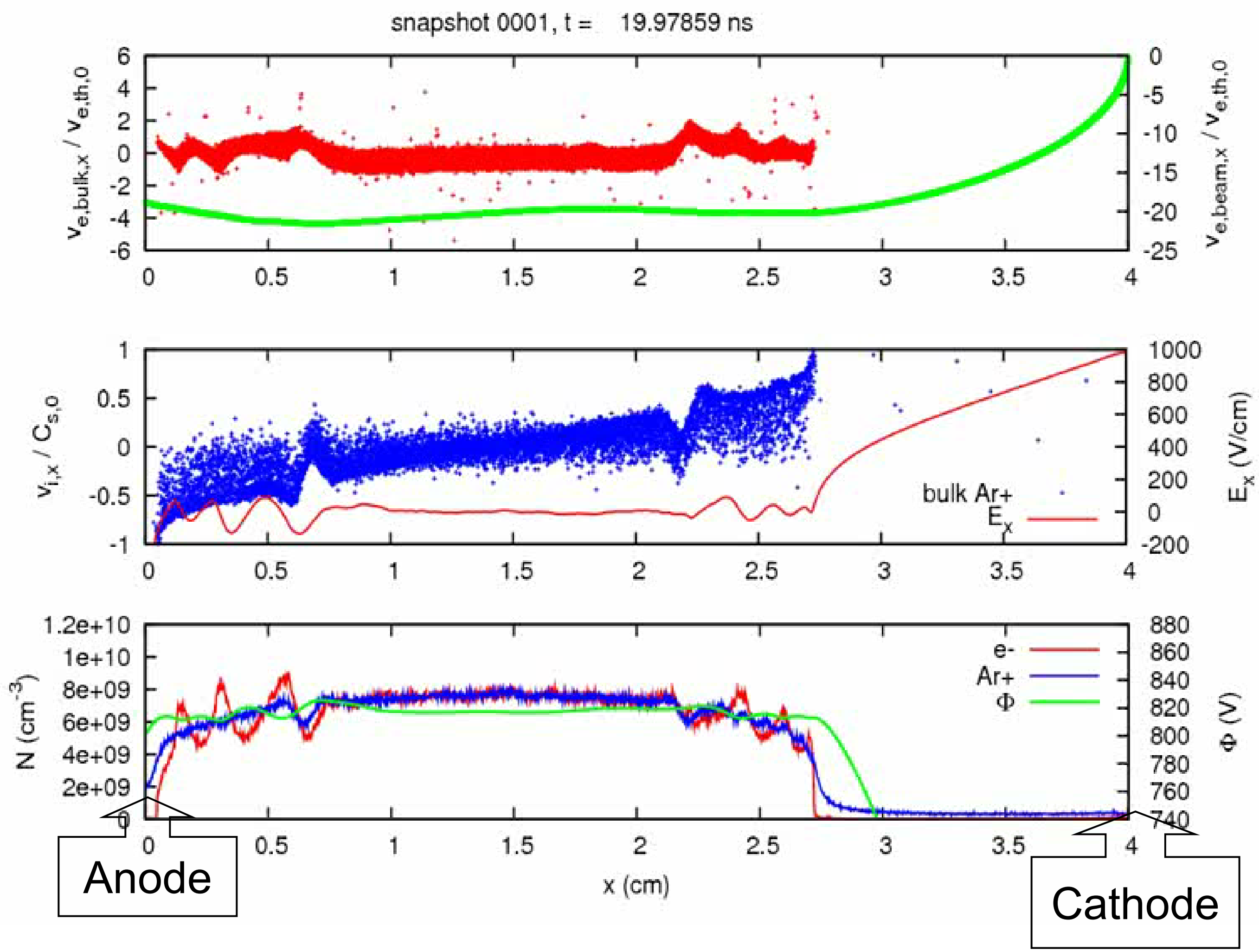

Electron velocity

Ion velocity

Density

red = bulk

green = beam

Electric field

Electro-static potential

Short-wavelength plasma waves appear in the density gradient region

Initial profiles of electron density (top) and electrostatic potential (bottom).

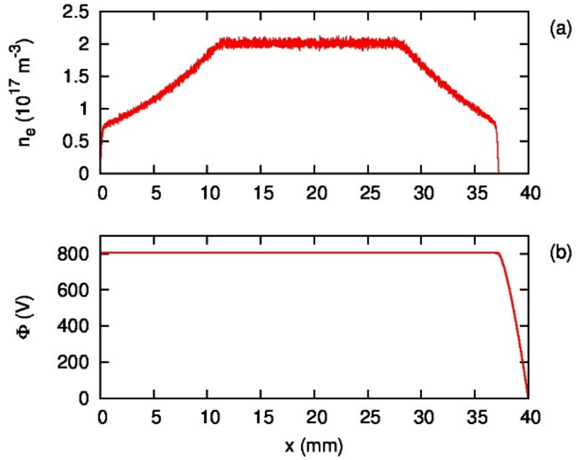

Cathode electron emission current 6.72 mA/cm2, relative beam density 0.000125.

Electric field vs coordinate (horizontal) and time (vertical).

Profile of the electric field at time marked by the arrow in the figure above. The anode is at x=0.

Amplitude of frequency spectrum of the electric field (color) vs the frequency (vertical axis) and coordinate (horizontal axis).

Electron plasma frequency (red) vs coordinate. The blue line marks the frequency excited by the beam.

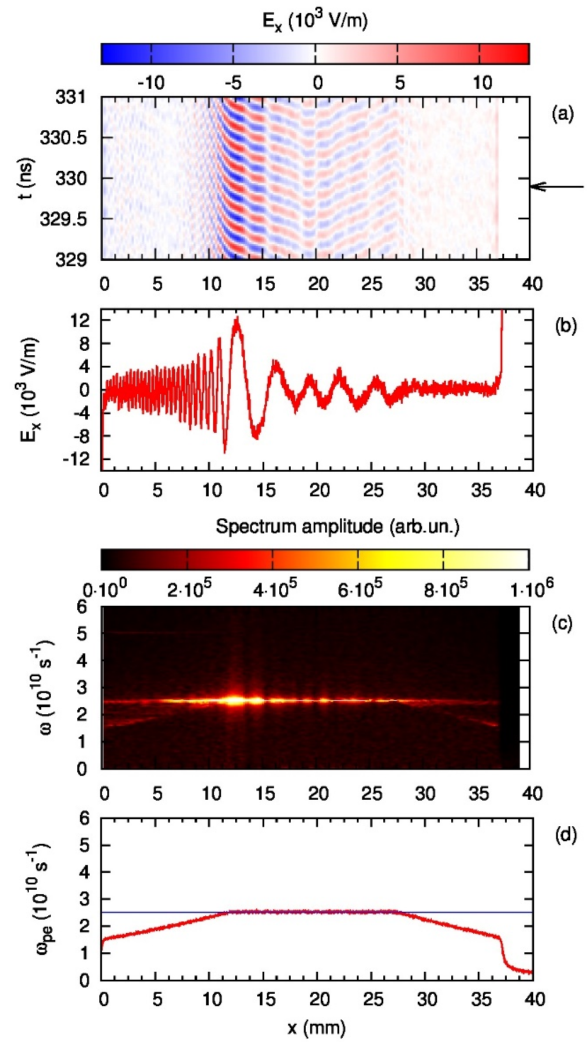

ELECTRIC FIELDS CAN REACH kV/cm WITH BEAM CURRENT OF 20 mA/cm^2

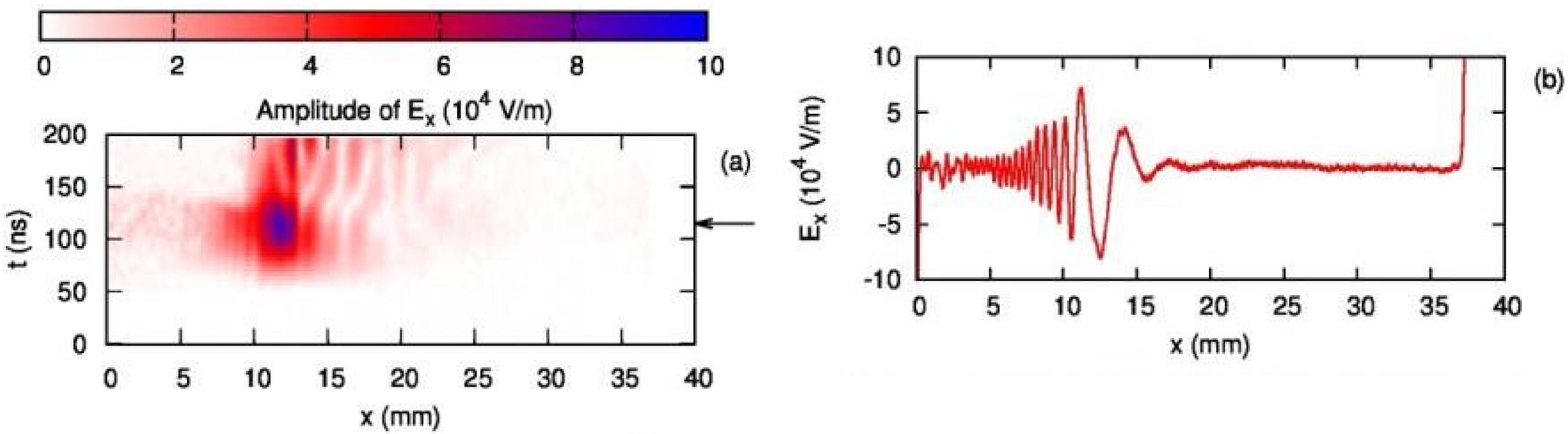

Now there is sufficient "kick" from the electric field to accelerate electrons out of the background.

PPPL PRINCETON PLASMA PHYSICS LABORATORY

UNIVERSITY OF ALBERTA

INTENSE LOCALIZED HF ELECTRIC FIELDS MAY BE A SOURCE OF MEDIUM-ENERGY ELECTRONS

Electron velocity

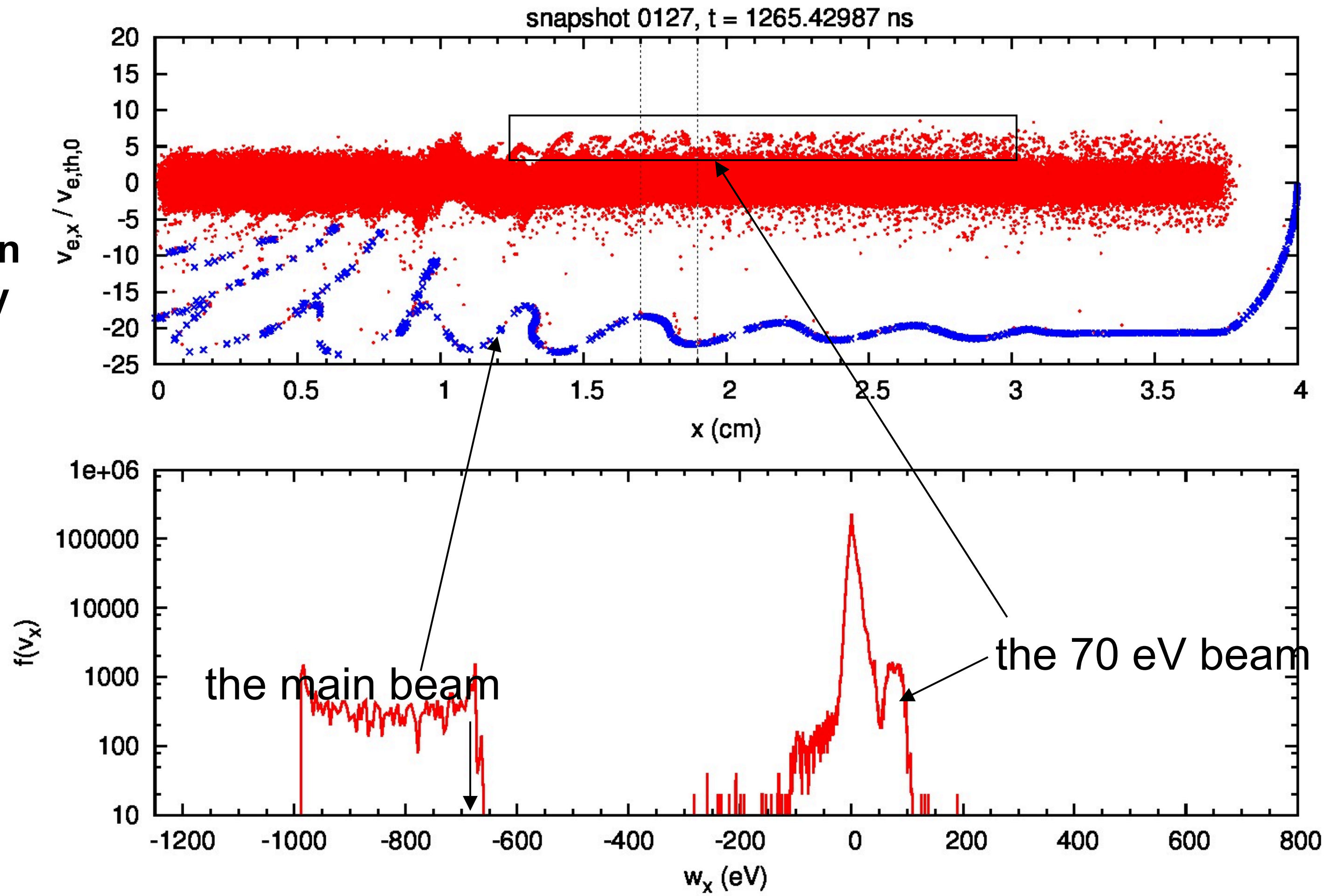

red = bulk

blue = beam

PPPL
PRINCETON PLASMA PHYSICS LABORATORY

UNIVERSITY OF ALBERTA

Mechanism of short-wavelength electron plasma wave excitation

Spectrum in k and w obtained for the electric field calculated in the simulation.

Theoretical dispersion: plasma wave in the density plateau (curve 1), plasma wave for density at x=5.9 mm (curve 2), the beam mode (curve 3), and the frequency excited by the beam (line 4).

$$\omega^2 = \omega_{pe}^2 + 3k^2 T_e/m_e$$

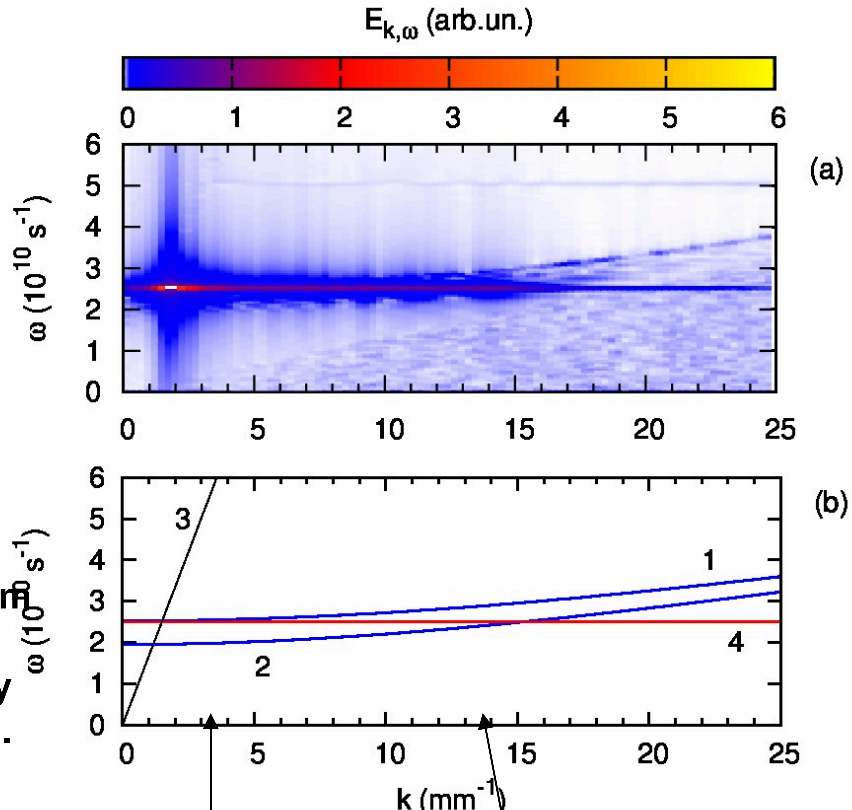

Wavenumber in the plateau area

Wavenumber in the density gradient area

The beam excites a strong plasma wave in the middle of the plasma.

The frequency of this wave defines the frequency of oscillations everywhere else.

In areas where the plasma density is lower, the wavenumber is larger, that is the wavelength is shorter.

Acceleration is the combination of short resonance, strong field, and non-uniform wave phase velocity and amplitude

Color map of the electric field vs coordinate (horizontal axis) and time (vertical axis).

Phase space energy-coordinate.

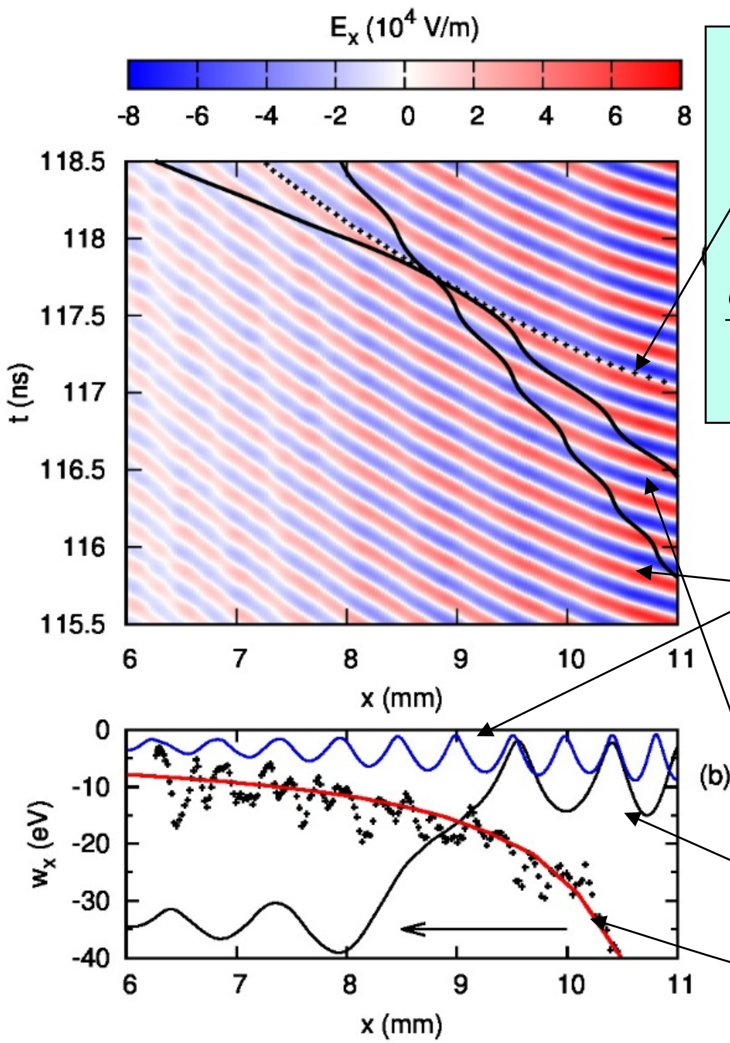

Phase speed of plasma wave calculated by differentiation of level lines (black markers) and theoretically (red curve).

$$\frac{\omega}{k}=\frac{\sqrt{3T_e/m_e}}{\sqrt{1-n(x)/n_0}},\ n_0-n(x)>>n_0\frac{3T_e}{2w_b}$$

Particle with initial energy 4 eV. No acceleration.

Particle with initial energy 7 eV.

The highest energy is acquired by recycled electrons

Color map of the electric field vs coordinate (horizontal axis) and time (vertical axis). Initial particle energy 6 eV.

First stage of acceleration.

Second stage of acceleration.

Phase space energy-coordinate.

O is the origin point, A is the first acceleration, B is the second acceleration, E – escape.

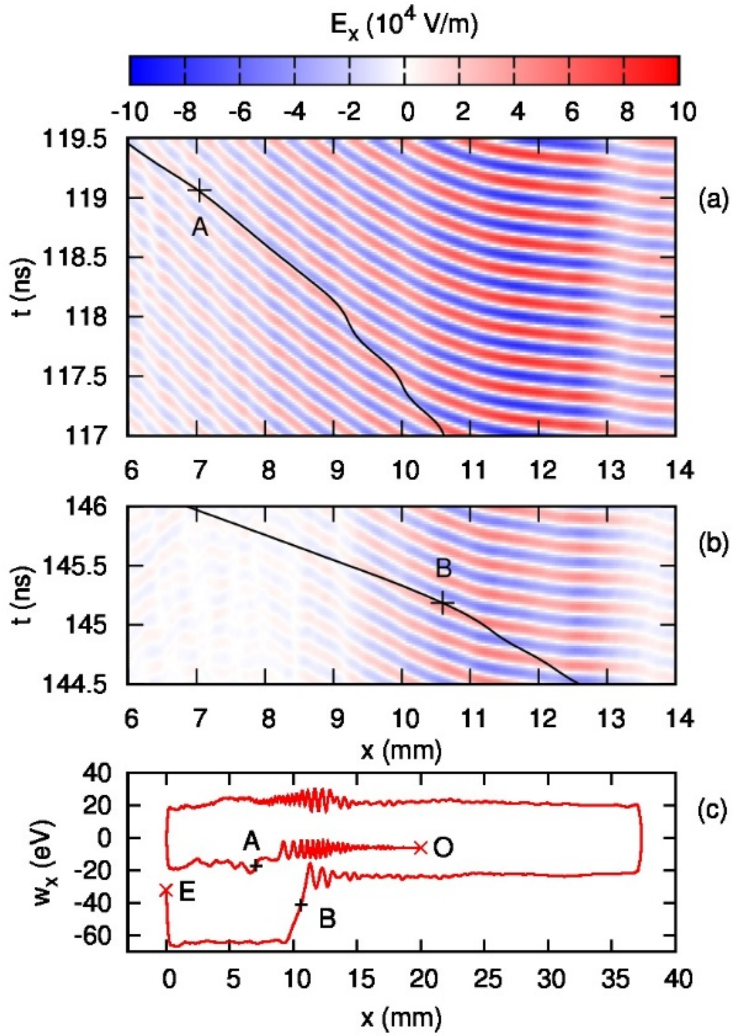

- Some electrons do not escape after the first acceleration.
- Such electrons make a round trip through the plasma and density gradient area with higher initial energy.
- They interact with the short waves in areas where the wave phase speed is higher, closer to the instability area.
- The energy after the second acceleration (~65eV) is an order of magnitude higher then the initial energy (~6eV).
- Such a mechanism explains why the highest energy suprathermal electrons appear with a delay.

Summary for beam-plasma interactions

- **We considered numerically the two-stream instability in a dc discharge with constant electron emission from a cathode.**
- **Plasma waves with short wavelength appear when a plasma wave excited by the beam enters a density gradient region with lower plasma density.**
- **The short-wavelength waves accelerate bulk electrons to suprathermal energies (from few eV to few tens of eV). Such acceleration is a one-time process and occurs along the direction of the wave phase speed decrease. It is possible because the wave phase speed and amplitude are strongly nonuniform.**
- **Some of the accelerated electrons may be reflected by the anode sheath and reintroduced into the density gradient area where they will be accelerated one more time. The energy of an electron after the second acceleration can be an order of magnitude higher than its initial energy.**
- **These processes may be relevant to observations of suprathermal (~100eV) peaks on the EVDF in a DC/RF discharge [Chen and Funk, 2010].**
- **The temporal growth rate and the amplitude of saturation of the instability are different functions of the beam density compared to the classical values obtained for infinite plasmas.**

Overall Conclusions

•Plasma processing is a multibillion dollar industry in revenues with inadequately funded fundamental research support.

•Semiconductor equipment requires precise control of plasma surface interaction. Partially-ionized plasmas allows for such control because of great availability in choices of electron, ion and photon energy distribution functions that can be designed and controlled according to required specifications.

•Industry will greatly benefit from innovative methods of designing electron, ion and photon energy distribution functions delivered to required surfaces.

•Examples of such innovative methods for crafting electron, ion and photon energy distribution functions have been recently developed by the DOE Center for Predictive Control of Plasma Kinetics.